

Centrifugal force reversal in the vicinity of a Schwarzschild black hole



Abeera Aleem
Regn.#NUST201463632MSNS78114F

A thesis submitted in partial fulfillment of the requirements
for the degree of **Master of Science**
in
Physics

Supervised by: Prof. Asghar Qadir

Department of Physics

School of Natural Sciences

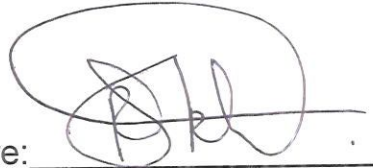
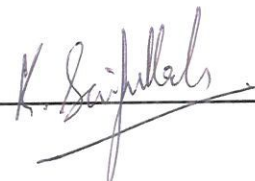
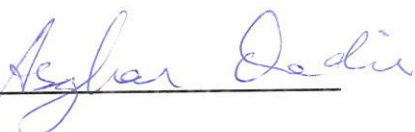
National University of Sciences and Technology

H-12, Islamabad, Pakistan

2018

National University of Sciences & Technology**MS THESIS WORK**

We hereby recommend that the dissertation prepared under our supervision by: ABEERA ALEEM, Regn No. NUST201463632MSNS78114F Titled: Centrifugal forcereversal in the vicinity of a Schwarzschild black hole be accepted in partial fulfillment of the requirements for the award of **MS** degree.

Examination Committee Members1. Name: Dr. Rizwan KhalidSignature: 2. Name: Dr. Muhammad Ali ParachaSignature: External Examiner: Dr. Khalid SaifullahSignature: Supervisor's Name: Prof. Asghar QadirSignature: Head of Department04/09/18

Date

COUNTERSIGNEDDate: 04/09/18Dean/Principal

THESIS ACCEPTANCE CERTIFICATE

Certified that final copy of MS thesis written by Ms. Abeera Aleem, (Registration No. NUST201463632MSNS78114F), of School of Natural Sciences has been vetted by undersigned, found complete in all respects as per NUST statutes/regulations, is free of plagiarism, errors, and mistakes and is accepted as partial fulfillment for award of MS/M.Phil degree. It is further certified that necessary amendments as pointed out by GEC members and external examiner of the scholar have also been incorporated in the said thesis.

Signature: Asghar Qadir
Name of Supervisor: Prof. Asghar Qadir
Date: 04/09/18

Signature (HoD): [Signature]
Date: 04/09/18

Signature (Dean/Principal): [Signature]
Date: 04/09/18

Dedication

*To my grandfather Mirza Nazir Baig Chughtai
and my beloved parents.*

Acknowledgements

In the name of Allah, the Most Gracious and the Most Merciful Alhamdulillah, all praises to Allah for the strengths and His blessing in completing this thesis and praise to Holy Prophet Hazrat Muhammad (P.B.U.H).

Special appreciation goes to my supervisor, Prof. Asghar Qadir, for his supervision and constant support. His invaluable help of constructive comments and suggestions throughout the thesis have contributed to the success of this research.

I would like to express my appreciation to my GEC members, Dr. Rizwan Khalid and Dr. Muhammad Ali Paracha for their support and help towards my postgraduate affairs. I would also like to acknowledge some special people at SNS who had been my constant support; a special thanks to Dr. Mubbashir Jamil and his Ph.D student Sumarna, who were there whenever I had to discuss anything related to GR. Dr. Shahid Iqbal and Dr. Aeysha Khaliq provided a great moral support.

I would like to express my gratitude to Dr. Muhammad Usman Sharif who helped me to get through my pre defence and my thesis. Special thanks to my best friends Affan Faisal, Faiqa Riaz, Hafsa Inam, Marya Zainab, Yusra Sohail, Sunia Javed and Zahid Iqbal, who have always been the friends in need. Some important people who made my journey easy at SNS were Tahir Zareef Kiyani Sahib, Mehfooz Hussain Sahib, Rub Nawaz Sahib, and Tanveer Sahib, I am obliged to them as well. I would like to give my profound gratitude to my mother for all her prayers, my father for being the one I could turn to every time I thought I was going to fail and my siblings for your kind words when they were really needed. To those who indirectly contributed to this research, your kindness and prayers means a lot to me.

Abstract

I have reviewed the centrifugal force reversal near a Schwarzschild black hole that was first proposed and explained by Abramowicz. There would be an expected centrifugal breakup near a neutron star but Abramowicz had proposed a mechanism which instead of providing centrifugal breakup, will bind the star better. The neutron star, thus, becomes stable rather than tearing apart. Here, the relativistic centrifugal force near a Schwarzschild black hole has been reviewed and we have not studied the breakdown near the neutron star. It can be studied for further research. This would take us forward, to see the problems related to the rotating fluid and its behavior near the strong gravitational fields.

Contents

1	Introduction	1
1.1	Energy Production in Stars	3
1.1.1	The Proton-Proton Chain	4
1.1.2	The CNO Cycle	5
1.2	Classification of Stars	5
1.2.1	Spectral Types of Stars	6
1.2.2	Hurtzsprung-Russel Diagram	6
1.2.3	Dwarf Stars	10
1.2.4	Compact Stars	10
1.2.5	Binary Stars	11
1.2.6	Variable Stars	19
2	Stellar Structure	24
2.1	Self-Gravitating Objects	24
2.2	Hydrostatic Equilibrium	25
2.3	Energy Transport	28
2.4	Equation of Thermal Equilibrium	32
2.4.1	Gravitational Instability and Mass Scales	33
2.5	Free-Fall Time	36
2.6	Scaling Relations on the Main Sequence	37
2.7	The Equation of State (EoS)	39
2.7.1	The Ideal Gas	40

2.8	Polytropic Models for Stars	41
3	Compact Stars	43
3.1	Degenerate Fermi Gas of Electrons	44
3.1.1	The Mass-Radius Relation	52
3.2	The Crab Nebula and Pulsar Detection	53
3.3	Neutron Stars	54
3.3.1	The Size of a Neutron Star	55
3.4	Heavy Progenitors	58
3.5	General Relativity	59
3.6	The Classical Black holes	63
3.7	The Relativistic Black Holes	64
3.8	The Schwarzschild Black Hole	64
3.8.1	Singularities of Schwarzschild Black Hole	67
4	Abramowicz's Relativistic Centrifugal Force	68
4.1	The Centrifugal Force Reviewed in Two Different Descriptions	69
4.2	Centrifugal Force in General Relativity	73
4.3	The Action of Centrifugal Force Reversal; The Rotosphere	81
4.3.1	The Effective Potential	86

Chapter 1

Introduction

“In the deathless boredom of sidereal calm, we cry with regret for a lost sun..”

Jean de La Vile de Mirmont, *L’Horizon Chimérique* 1920.

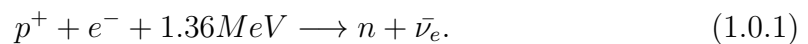
Astrophysics is a branch of science that uses the laws of physics in order to explain the birth, composition, life, and death of the stars, nebulae, galaxies and other stellar objects.

Stars change their composition slowly by fusing lower atomic number elements into higher ones. This process is called *stellar evolution*. The rate of stellar evolution varies with the mass of the star. A more massive star evolves faster because of the stronger gravity; the reason being the universal law of gravity that the amount of gravity a body possesses is proportional to its mass. The pressure and temperature increase as the pull of stronger gravity compresses the core of the star, which in turn increases the rate of fusion [1]. We will find the condition of hydrostatic equilibrium, which is required to balance the thermal pressure and the gravitational force of the star. The non-degenerate and degenerate equations of state of a star and the virial theorem will be discussed while explaining stellar structure.

Stellar objects include compact stars, which are said to be born from the ashes of luminous stars and are the most dense objects in the universe. The life cycle of stars is similar to the life cycle of humans, though the ages of stars depend on their masses. The death of massive stars, however, is much more dramatic. It can end

up in an enormous explosion and outshine an entire galaxy for several weeks. This is called a *supernova*.

Hydrogen burning is the first equilibrium state in stellar evolution. For this state, the star must have a minimum mass of $0.08 M_{\odot}$, where M_{\odot} is the solar mass $1.99 \times 10^{30} kg$. Stars lighter than this mass are called *brown dwarfs*. We will explain these stars in Section 1.2.3. During this whole period of hydrogen burning, the star is on the main sequence in the Hertzsprung-Russel diagram (discussed in detail in Section 1.2). When the fusion of hydrogen into helium is completed and the star runs out of hydrogen, it will contract and become even hotter with contraction. Here, nucleosynthesis and the virial theorem play their role for energy production in stars. After the main sequence phase, the core of the star continues to contract. The expansion of the outer layers of the star makes it a *red giant* star and the electron gas in the core becomes degenerate. The degeneracy pressure is able to withstand further contraction if $M \lesssim 0.5M_{\odot}$. Stars heavier than $6M_{\odot}$ attain a temperature $8 \times 10^8 \text{ }^{\circ}K$, at this point helium fusion sets in. But after this process, the depletion of helium causes further contraction of the star core and the fusion to carbon and then to oxygen continues. The star loses its enormous mass in these shell burning stages. Stars with an initial mass below $\sim 6M_{\odot}$ are said to lose enough mass, to bring it below the Chandrasekhar limit of $1.44 M_{\odot}$. These stars will end their life as *white dwarfs*. In cores, larger than the Chandrasekhar limit, the electrons that have established the electron degeneracy pressure would become ultra relativistic and the thermal pressure will not withstand the gravitational force. Unable to reach equilibrium, the star collapses. This marks the beginning of a neutron star. The core continues to collapse past the electron degeneracy state and the matter continues to heat up due to the release of potential energy, there is an inverse beta decay reaction in the core:



During this process, there seems to be a possibility that electrons can regenerate through beta decay because neutrons generated through such processes can be un-

stable. This does not happen. Following Pauli's exclusion principle, the degenerate electron gas has already filled all the available energy states and electrons less than 13.6 MeV energy cannot be formed. So, the generated neutrons are now stable. Further increase in energy enhances the inverse beta decay, which increases the neutrino emission. Meanwhile, the neutron degeneracy pressure has built up to halt the collapse and maintain an equilibrium. Before reaching the equilibrium state, if the core mass increases and exceeds the Chandrasekhar limit, then the star may collapse into a black hole. This collapse can also be possible due to the reversal of centrifugal force near a Schwarzschild black hole.

In Chapter 1, we will present the basics of Astronomy. Then, in Chapter 2, we will discuss stellar structure. In Chapter 3, the degenerate white dwarf stars and then the neutron stars degeneracy will be discussed. Chapter 4 will describe Abramowicz's relativistic centrifugal force where we will discuss the centrifugal force reversal near a Schwarzschild black hole.

1.1 Energy Production in Stars

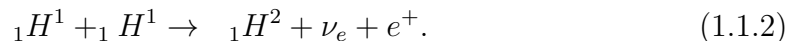
Nucleosynthesis is the process in which stars fuse lower atomic number elements into higher ones. Two chain reactions that are supposed to produce most of the heavier elements up to iron were considered by Hans Bethe in 1939 [2, 3]. Before explaining the two chain reactions, let's discuss what happens when the stellar core runs out of hydrogen, through the use of virial theorem:

$$E_t = -\frac{1}{2}(E_p) \quad ; \quad E_{tot} \equiv E_p + E_t = \frac{1}{2}E_p, \quad (1.1.1)$$

where E_t , E_p and E_{tot} are the thermal, potential and the total energies of the star, respectively ($E_p < 0$). Now total energy will decrease because the energy production through nuclear fusion diminishes. Hence, with the decrease in E_p , E_t increases. The stellar core contracts (E_p decreases), and the density and temperature will rise (E_t increases, adiabatic compression). The star spends half of the potential energy liberated in compression and the other half goes in the radiative losses.

1.1.1 The Proton-Proton Chain

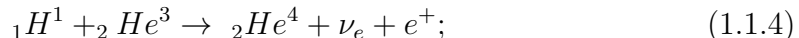
In the proton-proton chain reactions, four protons are utilized to form an alpha particle (helium nucleus). These reactions take place at a temperature of $\bar{T} = 15 \times 10^6 \text{ } ^0K$ (which corresponds to 13.6 eV , the ionization energy of hydrogen), in the central regions of the Sun. At such temperatures, the gases are completely ionized. This chain starts from two hydrogen nuclei, which interact to form an intermediate state and then, decays into a deuteron, an electron neutrino, and a positron [4], as follows



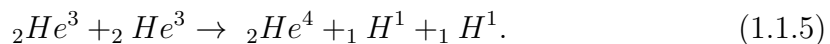
The ejected positron e^+ will find and annihilate any nearby e^- associated with one of the input hydrogens, to produce two photons $e^- + e^+ \rightarrow 2\gamma$, which are then absorbed to give translational energy to two atoms. The two gamma rays would have the energy of about $2m_e c^2$ i.e., 1.02 MeV [4]. This energy and the kinetic energy of the deuteron contribute to the internal thermal energy of stars.



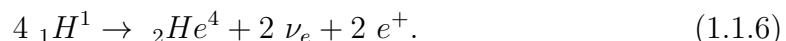
The striking photon with a deuteron gives an isotope of ${}_2He^3$ and a gamma. It may proceed now, in either two of the following reactions:



or



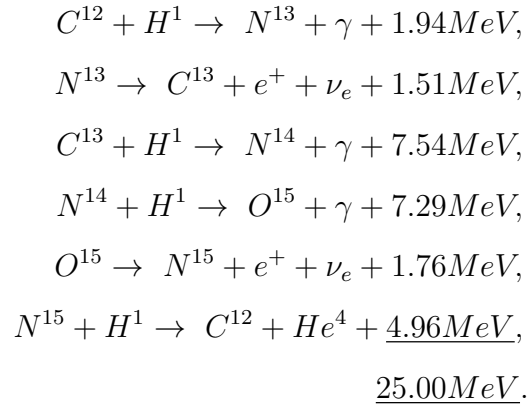
So, four protons synthesize to form a helium nuclei as follows



During all these reactions the conservation of charge, lepton number (the quantum number for the leptons i.e. e, μ, τ, \dots and their anti-particles) and baryon number (the quantum number for baryons, i.e. $n, p, \Lambda, \Sigma, \dots$) is conserved.

1.1.2 The CNO Cycle

Another route can be taken in the synthesis of helium. It is the Carbon-Nitrogen-Oxygen (CNO) cycle. The reactions of this cycle involve carbon, nitrogen and oxygen nuclei to create a helium nucleus from four protons. The process starts by making use of the carbon present in the core of the stars. This process occurs at higher temperatures of about \bar{T} [4]. In this process carbon, nitrogen and oxygen work as catalysts. The following six reactions occur [5]



The p-p chain is less sensitive to temperature as compared to the CNO cycle. At lower central temperatures ($T_c < \bar{T}$), the CNO cycle gets dominated by a p-p chain and in higher central temperatures the CNO cycles dominate over the p-p chain. The stars with mass $M < M_\odot$, p-p chain reaction becomes their main channel for energy production and for stars with masses $M > M_\odot$, the CNO cycle becomes their main source for energy generation [3].

1.2 Classification of Stars

The stars spread over the night sky are mostly *Main Sequence* stars. Like our Sun, these stars are burning hydrogen to helium in their cores. The classification of stars is based on their spectral characteristics and generation. Their spectra are basically the graphs of intensity plotted against the wavelength. In this section, we

will discuss some spectral properties and how the stars live on the main sequence according to Hertzsprung-Russel diagram.

1.2.1 Spectral Types of Stars

Stars are also classified based on their emission (a series of bright spectrum lines) or absorption (a series of dark spectrum lines) line spectrum. The absorption lines are related to the surface temperature of the star. Most of the stars are classified by temperature (spectral type) from hottest to coolest. The spectral type, based on the Morgan-Keenan (MK) system where O, B, A, F, G, K, M , run from the hot massive O stars with helium absorption lines to cool M stars with the metallic spectral lines, respectively [3]. These categories are further sub-divided into subclasses from 0 to 9, with A_0 to be hotter than A_1 and similarly, B_2 hotter than B_3 .

1.2.2 Hertzsprung-Russel Diagram

In 1911 two astronomers, Ejnar Hertzsprung and Henry Norris Russell, at Princeton University, independently plotted a graph showing a relationship between the logarithmic effective temperatures and the logarithmic luminosities of stars. On the x -axis (the horizontal axis) the quantity measuring the temperatures of the stars was plotted and the y -axis shows the quantity that measured the intrinsic brightness of stars. The diagram is known as the H-R diagram and is a very important analytic tool for the astronomers. The location of a star on the H-R diagram tells its luminosity, temperature, color, spectral type, mass, chemical composition and the evolutionary history.

Plotting these stars on the H-R diagram shown in Figure (1.1), the astronomers found that most of the stars were concentrated in a limited diagonal region rather than spreading out on the whole graph. Stretching from the upper left (hot O and B) to the lower right (cool and faint red M stars), this band contains almost 90 percent of the stars on it, that burn hydrogen in their cores. This band is called *main sequence* or *dwarf sequence*, extending from an absolute magnitude of about

-7 or -8 to +15 [6]. The temperature range is more than $3,000\text{ }^{\circ}\text{K}$ to $30,000\text{ }^{\circ}\text{K}$ and the luminosity and surface temperatures lie in this large range steadily.

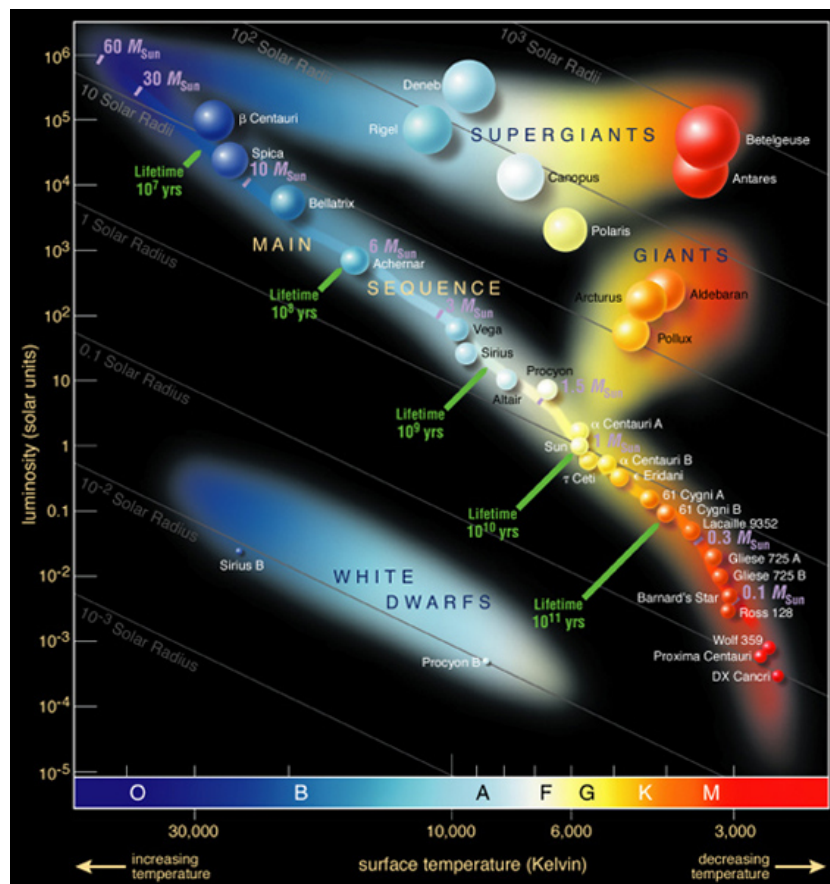


Figure 1.1: The H-R diagram (Courtesy ESO).

The luminous hottest stars lie on the upper left side of the diagram, thus the temperature increases from right to left. Also, since the brightest stars are on the top, magnitude decreases towards the top. The low luminosity and least massive, cool stars lie on the lower right side of the H-R diagram.

The Magnitude Scale

Hipparchus the Greek astronomer, recorded the brightness scale of stars. He ranked stars into magnitudes of 1 to 6, according to brightness. The first magnitude goes to the brightest star, second for the less bright and so on, till the sixth magnitude for

the dimmest stars. Modern measurements show that the difference between the first and sixth magnitude represents a brightness ratio of 100 ($100^{1/5} = 2.512$). Hence, each magnitude is 2.512 times brighter than the other [7]. The ratio of brightness of one object to the second can be given by

$$\frac{B_1}{B_2} = 100^{(0.2)(m_2 - m_1)}, \quad (1.2.1)$$

the magnitude m_1 of one object can be found by comparing its brightness by the brightness of an other object with a known magnitude (m_2). So

$$m_2 = m_1 + 2.5 \log_{10} \left(\frac{B_1}{B_2} \right). \quad (1.2.2)$$

How bright a star seems from the earth, depends upon its distance from the earth and its intrinsic brightness. The luminosity of a star is a measure of the total amount of energy that is radiated from its surface in one second. It is expressed in terms of the luminosity of the Sun and is measured by the star's *absolute total bolometric magnitude*. Thus, considering M_{bol} as the absolute magnitude and L the luminosity of the star, the following relation holds

$$M_{bol} - M_{bol\odot} = 2.5 \log \frac{L_{\odot}}{L}, \quad (1.2.3)$$

where $M_{bol\odot}$ and L_{\odot} are the Sun's bolometric magnitude and luminosity, respectively.

Radius and Luminosity of Star

The total luminosity or the bolometric magnitude of a star can be expressed in terms of effective temperature by the relation, one can also find the value of radius if the temperature of the stellar photosphere is known.

$$L = 4\pi r^2 \sigma T_{eff}^4, \quad (1.2.4)$$

where $4\pi r^2$ is the surface area of the star and σ is the Stefan Boltzman's constant. This relation (1.2.4), is known as the *Luminosity-Radius-Temperature relation* for stars and the temperature T_{eff} is known as the *effective temperature*. The effective

temperature can be defined as the temperature of a black body with the same energy flux at the surface of the star. This formula gives the amount of the total radiant energy passing per second through the entire surface of the star.

There exists another branch of stars with lower effective temperatures, high luminosity and larger radii extending from F to M spectral type, these occupy the upper right corner of the H-R diagram. These are called *giants*. They are intrinsically brighter than the main sequence stars because their luminosities are even larger than the stars of their spectral type.

Giants and Supergiants

Upwards to the right of the main sequence, the stars that fuse higher atomic number elements than hydrogen, are *giants*. These stars have relatively larger radii and are intrinsically brighter than other dwarf stars on the main sequence. Because of the larger radiating area, these *giant* stars are more luminous than the dwarfs of the same spectral classes and their absolute magnitudes range from -1.0 to +1.0. Then, above these giant stars, there are *super giants*, that are brighter than the giant stars. Within a sparse distribution, super giants have magnitudes ranges from -3.0 to -0.8.

Spectral lines can show different characteristics within the same spectral type or temperature. So, the second type of classification system for stars was devised using luminosity. Two stars with similar effective surface temperatures but different luminosities must differ in size.

Luminosity Classes

Stars can also be divided into luminosity Classes I-V on the H-R diagram. The complete classification of stars can be obtained by specifying both the luminosity and the spectral type classes. Class I stars are called *supergiants*, Class II and III stars are *giants*, Class IV stars are *subgiants*, Class V stars are *dwarfs*.

1.2.3 Dwarf Stars

Small faint objects, that lie below (to the lower left corner of) the main sequence, of the classes from middle *B* to *G* with absolute magnitudes ranging from +10.0 to +15.0, are called *white dwarf* stars [1, 7]. Then, there are small hot stars, containing few elements heavier than helium and having lower luminosity than the *main sequence* stars of similar temperature or same spectral type, these are the *sub dwarfs*. The region in the diagram between the main sequence and the giant branch, which is free from stars, is called the *Hertzsprung gap*.

Brown Dwarf Stars

Those astronomical objects that are less than the minimum mass for a star are called brown dwarfs. These bodies are too small to become stars as they would never develop enough pressure, density and high temperature (\bar{T}), to initiate hydrogen fusion in the core of the star. They are too large to be regarded as planets. Before reaching this mass limit, the compression and gravitational balance continue to cause radiation to the point where its virial temperature becomes equal to the microwave background temperature when it will be in equilibrium. This equilibrium condition will halt any further compression because now the potential will be at its minimum between any pair of atoms, so no further collapse is possible and the star at this point becomes non-radiating.

These stars are labeled with spectral types *L* and *T*. In order to observe these stars infrared telescopes are used.

1.2.4 Compact Stars

Compact stars are said to be the last stage of the stellar course. When all the elements up to iron get exhausted in nucleosynthesis, these stars are left with a sea of electrons in their core. They remain stable, by balancing the gravitational pressure with the Fermi degeneracy pressure of electrons [1].

Any star with a mass between 3 and 10 M_{\odot} will become a red giant with a

white dwarf core, in about a million years, then eject the outer part and become a neutron star [8]. *White dwarf* star is a small $\sim (0.002-0.08)R_{\odot}$ (where R_{\odot} is the solar radius $6.95 \times 10^8 m$) dense star [9], with mass less than the Chandrasekhar limit i.e, $M_{ch}=1.4M_{\odot}$ (and for a cold star this limit is $M_{ch}=0.7M_{\odot}$). The Chandrasekhar mass is the maximum stellar mass that can be supported by degenerate electron pressure [10].

When a white dwarf has cooled down to the temperature of the cosmic background radiation, it would not radiate energy or emit light. Now, it would become a cold dwarf star known as *black dwarf*.

The stars with a mass between $1.4-3.2M_{\odot}$ and a radius of $10 km$ are *Neutron stars*. For masses greater than the critical mass (of $3.2 M_{\odot}$), a neutron star in a binary system must become a black-hole [8]. Neutron stars are formed from the massive stars that are energetic enough to fuse elements up to iron. When iron is formed, it gets deposited in the core and a rapid increase in density starts which, in turn, contracts the core inwards. The rise in temperature, due to this whole activity and the increased density, allows electron capture in the core.



Neutron stars are extremely dense objects, their gravity is strong enough to significantly bend light, from another star, in a process known as *gravitational lensing*. The supernova explosion which is the cause of the formation of a neutron star gives it a rapid rotation. Neutron stars are found spinning with extreme magnetic fields known as *pulsars* or *magnetars*.

1.2.5 Binary Stars

Stars that do not travel alone but have one or more gravitationally bound companion with them are called star systems. These stars orbit around their common center of mass. Binary systems allow the direct measurement of mass. In order to examine, how such systems determine the mass, there is a need to explore some aspects of the Keplerian two-body problem, which explains the motion of two stars that are

orbiting around their common center of mass in elliptical trajectories. The two orbiting masses have the center of mass where

$$r_1 m_1 = r_2 m_2, \quad (1.2.6)$$

where a is the separation between the masses, $a = r_1 + r_2$,

$$r_1 = \frac{m_2}{m_1} (a - r_1), \quad (1.2.7)$$

or

$$r_1 = \frac{m_2}{m_1 + m_2} a \quad \text{and} \quad r_2 = \frac{m_1}{m_1 + m_2} a. \quad (1.2.8)$$

From these two masses, each is subjected to a mutual gravitational attraction and orbit around their common center of mass with an angular frequency ω . So, the equation of motion for the first mass comes out to be,

$$m_1 \omega^2 r_1 = \frac{G m_1 m_2}{a^2}, \quad (1.2.9)$$

where G is the gravitational constant and $\omega = 2\pi/P$, now substituting r_1 from equation 1.2.8, this becomes Kepler's law:

$$\omega^2 = \frac{G(m_1 + m_2)}{a^3}. \quad (1.2.10)$$

This law can be used to deduce the stellar masses, as in the case of the Sun. In above equation $P = 2\pi/\omega$ is the orbital period, which is 1 year for the Sun. The mass of the Earth is taken negligible as compared to the Sun. The above equation becomes

$$M_\odot \approx \frac{\omega^2 a^3}{G} = \frac{4\pi^2 a^3}{P^2 G}, \quad (1.2.11)$$

$$M_\odot = \frac{4(3.14)^2 (1.5 \times 10^{11} m)^3}{(3.15 \times 10^7 s)^2 (6.67 \times 10^{-11} m^3 kg^{-1} s^{-2})} = 2.0 \times 10^{30} kg. \quad (1.2.12)$$

Visual Binary

A visual binary is a system of two or more stars that which are resolved as individual stars with the use of a telescope. In the visual binary, the mass of each component

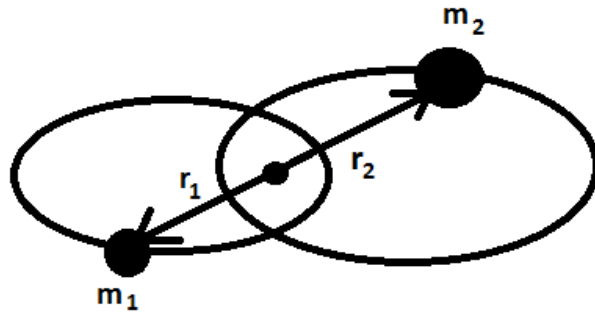


Figure 1.2: A binary system with masses m_1 and m_2 orbiting in circle at their common center of mass, with radii r_1 and r_2 from their common center of mass, respectively.

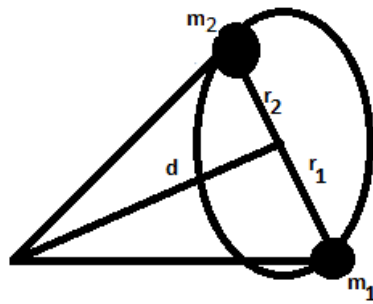


Figure 1.3: A binary system with masses m_1 and m_2 orbiting in circle at their common center of mass, at a distance d , with radii r_1 and r_2 from their common center of mass, respectively.

can be found. Consider two stars with masses m_1 and m_2 , orbiting around their common center of mass.

$$\frac{m_1}{m_2} = \frac{r_2}{r_1} = \frac{a_2}{a_1}, \quad (1.2.13)$$

where r_1 and r_2 are the distances from the common center of mass and a_1 and a_2 are the semi-major axis of the elliptical orbit (referring to Figure (1.2)). If the distances r_1 and r_2 subtend angle $\theta_1 = r_1/d$ and $\theta_2 = r_2/d$ at the star's distance d (Figure (1.3)), then the mass ratio becomes

$$\frac{m_1}{m_2} = \frac{\theta_2 d}{\theta_1 d} = \frac{r_2}{r_1}. \quad (1.2.14)$$

If d is known then we can deduce individual masses using Kepler's law.

$$P^2 = \frac{4\pi^2 a^3}{G(m_1 + m_2)}. \quad (1.2.15)$$

From the measurement of the period P which is the same for both orbits and the semi-major axis $a = a_1 + a_2$ of the binary stars, the sum of the masses of the stars can be obtained.

Spectroscopic Binary

While studying the spectrum of a star, the spectral lines oscillate periodically about the average wavelength. The variations in the spectrum (which is the resultant we get from the superposition of the spectral features of two stars) are caused by the Doppler shift [7]. When the star, while moving in its orbit appears to come towards the observer, a shorter wavelength will appear and when it moves away from that observer, longer wavelength is appears. In a double-lined spectroscopic binary, the maximum blue and red shifts we measure are the lower limits of the true velocities. This is because of the unknown inclination i of the orbital plane to the line of sight. The true orbital and the Doppler velocity amplitudes are related as

$$v_{1r} = v_1 \sin i \quad ; \quad v_{2r} = v_2 \sin i. \quad (1.2.16)$$

When the eccentricities are small $\epsilon \ll 1$, the orbital speed becomes a constant i.e. $v = 2\pi a/P$, where P is the period and the semi-major axis a is now the radius.

Substituting in equation (1.2.13) we get

$$\frac{m_1}{m_2} = \frac{Pv_2/2\pi}{Pv_1/2\pi} = \frac{v_2}{v_1}, \quad (1.2.17)$$

or, in terms of observables,

$$\frac{m_1}{m_2} = \frac{v_{2r}/\sin i}{v_{1r}/\sin i} = \frac{v_{2r}}{v_{1r}}. \quad (1.2.18)$$

Thus, the mass ratio can be deduced independently of the unknown inclination, same as in the case of visual binary. However, in order to find the sum of the masses of a spectroscopic binary we require the inclination angle i , by replacing a with $a = a_1 + a_2$ in (1.2.15), we get

$$a_1 + a_2 = \frac{P}{2\pi}(v_1 + v_2). \quad (1.2.19)$$

Substituting this in equation (1.2.15) and solving for the sum of masses we obtain

$$m_1 + m_2 = \frac{P}{2\pi G}(v_1 + v_2)^3, \quad (1.2.20)$$

this sum of masses in terms of observables become

$$m_1 + m_2 = \frac{P}{2\pi G} \left(\frac{v_{1r}}{\sin i} + \frac{v_{2r}}{\sin i} \right)^3, \quad (1.2.21)$$

or

$$m_1 + m_2 = \frac{P}{2\pi G} \frac{(v_{1r} + v_{2r})^3}{\sin^3 i}. \quad (1.2.22)$$

When the spectrum of one of the stars in the pair is observed the periodic variations indicate the presence of an unseen companion star, this is a single-lined spectroscopic binary. This might happen when one of the stars in the binary is much fainter than the primary star i.e, a compact star (a neutron star or a black hole). Another possibility occurs, if the companion (faint star) is a planet. In either of these cases above, a single-lined spectrum is obtained. By studying this spectrum, we will not be able to measure v_{2r} , but we can substitute the relation (1.2.18) in equation (1.2.22) to obtain

$$m_1 + m_2 = \frac{P}{2\pi G} \frac{(v_{1r} + v_{1r}m_1/m_2)^3}{\sin^3 i}, \quad (1.2.23)$$

or

$$m_1 + m_2 = \frac{P}{2\pi G} \frac{v_{1r}^3}{\sin^3 i} \left(1 + \frac{m_1}{m_2}\right)^3. \quad (1.2.24)$$

This can be rearranged in the following form

$$\frac{m_2^3}{(m_1 + m_2)^2} \sin^3 i = \frac{P}{2\pi G} v_{1r}^3. \quad (1.2.25)$$

If the mass of one of the companion stars is unknown, then from the left hand side of this equation, we can get the mass m_1 of the unseen component. If the condition $m_2 \ll m_1$ is satisfied, which happens in cases where secondary component of a spectroscopic binary is a planet, then $m_1 + m_2 \approx m_1$. Substituting ($m_1 + m_2 \approx m_1$) in equation (1.2.25) we get

$$m_2^3 \sin^3 i = \frac{P}{2\pi G} v_{1r}^3 m_1^2. \quad (1.2.26)$$

The above relation can be used in order to find extra-solar planets.

Interacting Binary

Before discussing the interacting binaries, there are three possible cases which can be discussed. In the first case, we have stars that are close and gravitationally bound but can only interact through the light. This interaction appears to be very slow as no matter flows from one star to the other. In the second case, the stars are like our Sun, where the solar winds can take the matter with them. This case has its own limitations because this case includes self-interaction but such stars have not studied yet. Third, is the case of a binary system where one of the stars is a collapsed star and is gravitationally bound to the companion normal or giant star. Both the stars are lying so close that the collapsed star can accrete matter from its companion giant star. Further process and details will be discussed in this section.

Some stars are powered by the accretion of matter onto a gravitational potential well from companion stars. This category includes interacting binaries, pre-main sequence stars, quasars and possibly some supernovae or gamma-ray bursts. These stars are not the normal luminous stars that survive through nuclear burning [10].

The spin axis and orbital plane axis of the stars with circular orbits are aligned parallel to each other. Each star completes a single rotation about its axis once per orbit, in this way, each star will always see the same side of one another. At small distances, the action of tidal forces exerted by stars on each other can be observed. Consider the action of a force which is exerted on the mass element m on the surface of the star at Δr from the center, which is due to the star of mass M_1 itself,

$$F_{grav} = -\frac{GM_1m}{\Delta r^2}. \quad (1.2.27)$$

Now, the tidal force on this mass element due to the star M_2

$$F_{tidal} = -GM_2m\left(\frac{1}{r^2} - \frac{1}{(r + \Delta r)^2}\right), \quad (1.2.28)$$

now assuming $\Delta r \ll r$,

$$F_{tidal} \approx \frac{2GM_2m\Delta r}{r^3}, \quad (1.2.29)$$

then the ratio comes out to be

$$\frac{F_{tidal}}{F_{grav}} = 2\frac{M_2}{M_1}\left(\frac{\Delta r}{r}\right)^3. \quad (1.2.30)$$

The fraction $\Delta r/r$ gives us the distortion of shapes of the stars, if the factor $\Delta r/r$ is large, stars will have large distortions. The distorted shape may come up to be two ovals pointing at each other in such a way that they make a horizontal 8. There are two phases; the tidally locked phase and is not tidally locked yet. Tidal locking is the phenomena which occur when an object's orbital period matches its rotational period [10].

In this phase, when stars are not tidally locked, the orbiting stars may lose energy due to friction during shape deformation of stars.

Once the tidally locked state is attained, the state seemed to be stationary in the reference frame of the rotating binary system at the same frequency. For a specific isopotential surface, the stars form crossed lobes which connect at a single point between the two stars, making a figure 8 (referring to Figure 1.4). These

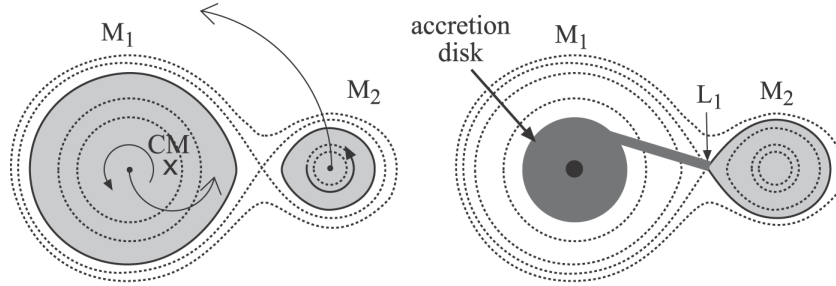


Figure 1.4: The figure on the left side, shows the interacting binaries, where the dotted curves show the equipotential surfaces, in the co-rotating reference frame of a binary system. The figure on the right side shows two stars (primary at left and secondary at right) where the secondary star fills its Roche lobe. The matter flows through the point L_1 and falls onto the primary. The primary star now becomes a compact star [10].

are called *Roche Lobes*. The point where the lobes connect is known as the *first Lagrange point*, L_1 (Figure (1.4)). It is defined as the equilibrium point because the gravitational forces of the two stars and the centrifugal forces in the rotating frame, due to the rotation about the center of mass, sum up to zero. There are three possible interacting binaries if the matter falls onto the companion through the Roche lobe: the *detached binary*, neither of the stars fill the Roche lobe and both are spherical in shape; the *semi-detached binary*, one of the stars fills the Roche lobe and the stars are egg-shaped; the *contact binary*, both the stars fill their Roche lobes, simultaneously and connect physically through the point L_1 .

Now, discussing the third case where the stars are relatively closer than the other two cases. The observer in the inertial reference frame will observe that the angular momentum of the accreted matter and system's orbital angular momentum will have the same direction. In rotating reference frame this accreting matter when falling on the receiving star, will experience a Coriolis force. A compact (receiving) star will not take up the accreted matter directly onto its surface but the accreted matter will rather start orbiting the compact star making an *accretion disk* around it.

1.2.6 Variable Stars

The brightness of variable stars fluctuates either regularly or irregularly with respect to time. The plot exhibiting the brightness of a star (its magnitude) versus time is called a *light curve* [1, 7]. The comparison of light curves at different wavelengths can be of great use i.e, to find the physical properties of emitting sources.

Change in the brightness of a star as we have studied earlier might be caused due to the presence of its companion star eclipsing around the star under consideration. But individual stars can vary in brightness on their own. The brightness of a star is dependent on extrinsic or intrinsic factors. So variable stars may be divided into two broad groups: (a) extrinsic variables (b) intrinsic variables. Intrinsic variables can further be divided into two categories: (1) pulsating variables, (2) exploding and eruptive variables.

Eclipsing Binary

The eclipsing binary is a type of an extrinsic variable star whose luminosity changes due to the stars eclipsing around each other [7]. Algol's brightness varies periodically with a period of about 3 days. When the spectrum of Algol was read, it became clear that it was not a single star as considered before but an eclipsing binary. When the second star blocks the first or re-emerges forming an eclipse around it, a change in the brightness of the star occurs relative to an observer. The amount of time required for the stars to orbit around each other is the *binary period*. Above mentioned are the conditions under which eclipses are possible. When the binary's orbital plane and the line of sight are perpendicular to each other, no eclipse occurs. The eclipse is total or annular when the line of sight and the orbital plane are lined up to each other. The probability of partial eclipses is more than the above-mentioned cases, which may occur when both orbital plane and line of sight are inclined to any other angle [6].

A light curve is obtained in order to classify a system as an eclipsing binary. From the detailed observations and calculations of this light curve, the astronomers

may get the orientation, eccentricity and the inclination of the star.

When the smaller of the two stars move behind its companion bigger star, it is occluded and light is reduced, which can be exhibited on the light curve. Now, it is the light from the bigger star which can only be observed by the observer. There might be two eclipses that can be observed, *Primary* and *Secondary* (based on their spectral type which is the measure of temperature or stellar color). This determines that the energy outflow per unit area from the stellar surface as explained by the Stefan Boltzmann's law, $L \propto T^4$ in the blackbody. The hotter star radiates more energy per unit area than the cooler star. So, when the hotter is occluded by the cooler than this is a primary eclipse as more flux is being blocked than in the case of the cooler star being eclipsed by the hotter, which is the secondary eclipse.

The stars in the binary may be compared with respect to their brightness, less bright and the more bright stars. The star that outshines more than the other star in a binary system is called the primary and the other star is the secondary. The companion of Sirius A that is 10^4 times fainter than Sirius-A was found, which is a white dwarf, Sirius-B.

Intrinsic Variable Stars

The luminosity of a star changes due to internal changes; its contraction or expansion, throughout its life [7].

In a normal star, variations occur due to some flares or in some cases due to the accretion of matter from a companion star. This can also occur due to the variations in the intensity of the star, caused due to microlensing. Another case is the presence of unstable stars that pulsate in a rhythmic manner. These pulsations are observed by the periodic variation of light that they emit. The most well-known stars of this kind are Cepheid variables that have very stable pulsation periods.

Cepheid Variable Stars Cepheid stars are a type of intrinsic variable stars. In comparison to the stellar evolution time scales (which run into millions and billions

of years), these stars are relatively fast in periods, from days to months [11]. These stars regularly pulsate in size. This pulsating results in the changing brightness of these stars with a clock like regularity [12]. The period of Cepheid stars varies in a direct proportion to their absolute luminosities (brightness). The distance of such stars can be measured by comparing the apparent and absolute luminosities. The decreasing size increases the brightness and vice versa. The change in internal pressure may cause the effect of expansion and contraction of these pulsating stars. Various pulsating theories were presented but a Russian Astrophysicist claimed that these mechanical Cepheids can be maintained by pumping energy in the critical zone of ionization of some element. His investigations revealed that hydrogen ionization fails to excite such auto-pulsations due to the non-adiabatic nature of oscillations [6]. It was suggested that in the inner regions of the star, an ionized helium layer is present, which is compressed by the outer layers. When this ionized helium is compressed, it becomes opaque and in turn starts absorbing radiations from the core. This increases internal pressure due to the increased temperature and the star starts expanding outwards. The pressure is released as the star expand, thus, allowing the star to start this procedure again. The layer of ionized helium cannot be defined, where exactly it lies, but it cannot be too close to the core or to the photosphere otherwise, the star will not pulsate [7].

Exploding Variable Stars

The type of variable stars which flare up suddenly and sometimes explode are the Novae and Supernovae. Novae undergo occasional outburst, these are generally faint sub-dwarf stars that suddenly flare up to high luminosities.

Novae At the time of an outburst, the luminosity of a star becomes a million times greater than that of the original star. The total energy emitted in a nova is $\approx 10^{46}$ erg. There are also some novae whose outburst repeat after some years, these are known as *recurrent novae*. Kukerkin and Parenago derived a formula which relates the time-interval P and the amplitude A between two consecutive maxima

of a recurrent nova [6]

$$A = 0.80 + 1.667 \log P. \quad (1.2.31)$$

Supernovae The explosive death of a star is a Supernova, in which the cores of massive stars have burned everything into iron and nickel. The nuclei of stars heavier than nickel were thought to be formed in these explosions. Muslims from Baghdad, Chinese, South Americans and many others observed the nova in 1054 A.D, now recognized as a Supernova named by Zwicky and Baade in 1934 [5]. It was seen that there was an abrupt increase in the brightness of a star undergoing Supernova explosion and this brightness may increase by 20 more magnitudes [13]. Any star whose mass exceeds Chandrasekhar limit of $1.4 M_{\odot}$ can explode as a supernova. The total energy emitted in a supernova explosion is $\gtrsim 10^{51}$ erg.

Types of Supernova Supernovae are extremely bright explosions having -17 average absolute magnitude. These can be defined in two types: *Type I*; *Type II*.

Type I Supernova The *Type I* supernovas are characterized by the absence of hydrogen lines in their spectra whereas, the *Type II* supernovas do show prominent hydrogen spectra. As explained earlier, in an interacting binary, a dwarf star accumulates matter from its companion massive star. When the dwarf star gets enough mass which is needed to start the fusion of carbon, the reaction starts in the core. This builds a pressure and the core starts pushing it outwards. At the point when the outward fusion achieves enormous speed, exceeding the speed of sound, the star explodes [13]. This is also known as *Thermonuclear Supernova*.

Type II Supernova It occurs only in spiral galaxies, near the spiral arms. Unlike *Type I*, these explosions are due to the death of a single star, when a massive star ($8-12 M_{\odot}$) burns out all the fuel present in its core and reached the endpoint of stellar evolution, it explodes. The nuclear burning of lower atomic number elements to higher atomic number elements can take some years, oxygen and magnesium

burning could take 10^3 years, whereas, to burn silicon and sulfur into iron, it will take a few days, only. These are also called *Core – Collapse Supernovae*.

Chapter 2

Stellar Structure

The stellar structure explains basic rules and phenomena, on which the star's whole lifespan depends. In this Chapter, I am going to derive and explain basic equations, theorems, and equilibrium conditions, governing stellar structure.

2.1 Self-Gravitating Objects

A star can be defined as an object that radiates energy from an internal source and is bound by its own gravity. The potential energy of a self-gravitating body with mass M and radius R is $U \approx -(GM^2/R)$. If this body is in equilibrium through the balance of gas pressure and gravity, the virial theorem implies that it will have a temperature $T \approx (GM^2/R)$, that is, $T \approx (GMm_p/k_B R)$, where m_p is the mass of the proton ($1.672 \times 10^{-24} g$) and k_B is the Boltzmann constant (1.380×10^{-16} erg K^{-1}). For a sufficiently large value of M/R , this temperature can be high enough to ignite nuclear reactions at the core of the body. The nuclear energy generated near the core will be transported by radiation and convection towards the outer layers and will eventually escape the body. This will establish a temperature gradient in the body such that in steady state, the energy produced by the nuclear reactions is equal to the energy radiated by the star [9].

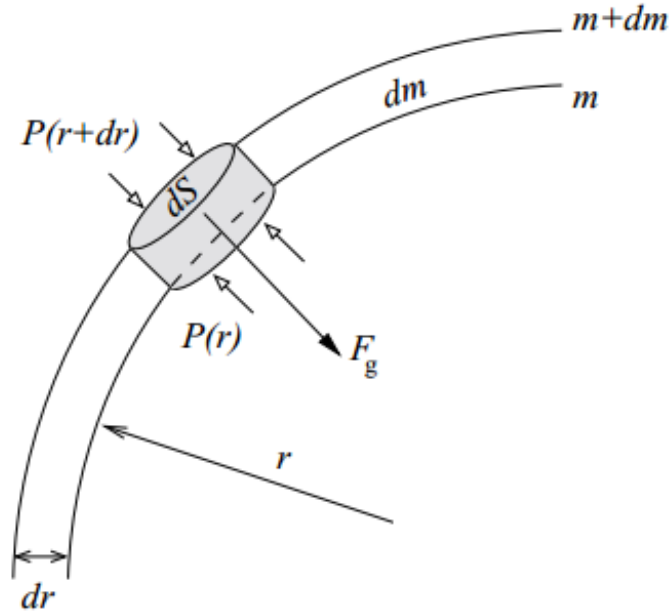


Figure 2.1: The figure shows a spherically symmetric system of radius r and mass m . The arrows show the acting forces, i.e. the gravitational force acting inwards and the pressure acting outwards.

2.2 Hydrostatic Equilibrium

To understand the equilibrium conditions, let us first see the collapse criterion. Stars form from the diffused interstellar gas and as the clouds contract to the density where nuclear burning starts, it must overcome the thermal pressure [4].

Equilibrium Condition

Consider a spherically symmetric shell of radius r and thickness dr , concentric within the star of radius R and mass M . These two are the only forces acting on the system, the self-gravitational force, and the internal pressure. The mass density and pressure at the distance r is $\rho(r)$ and $P(r)$, respectively as shown in Figure (2.1). Let $T(r)$ be the temperature and $L(r)$ be the luminosity at r , i.e. total energy radiated from

the surface of the star at r .

$$L(r) = 4\pi r^2 F(r), \quad (2.2.1)$$

where $F(r)$ is the flux density per unit area. The mass gradient inside the spherical shell can be obtained from the mass differential.

$$[(m + dm) - m] = 4\pi r^2 dr \rho(r). \quad (2.2.2)$$

Therefore, we have the equation of continuity as,

$$\frac{dm(r)}{dr} = 4\pi r^2 \rho(r), \quad (2.2.3)$$

which acts as the gravitational mass, located at the center and gives rise to an inward acceleration,

$$g(r) = \frac{Gm(r)}{r^2}. \quad (2.2.4)$$

Now, considering the pressure gradient that is required to balance the gravitational force.

The difference of the pressures of the inner and the outer surfaces balance out the weight of the spherical shell.

$$4\pi r^2 [P(r) - P(r + dr)] = \frac{4\pi r^2 G \rho(r) dr dm(r)}{r^2}, \quad (2.2.5)$$

or

$$\frac{dP(r)}{dr} = -\frac{Gm(r)\rho}{r^2}, \quad (2.2.6)$$

which is the equation of *hydrostatic equilibrium*. The pressure of the gradient is negative to counteract gravity. It decreases, as we move outwards due to increasing radius. If this equation holds at all radii, then our entire star system is in hydrostatic equilibrium. In that case we can find out a relation that can relate average internal pressure to the gravitational energy. Multiply both sides by $4\pi r^3$ and integrate from $r=0$ to $r = R$,

$$\int_0^R 4\pi r^3 \frac{dp}{dr} dr = - \int_0^R \frac{Gm(r)\rho(r)4\pi r^2}{r} dr. \quad (2.2.7)$$

The right side of above equation shows the gravitational potential energy of the star.

The energy gained by the star during its own formation

$$E_{gr} = - \int_{m=0}^{m=M} \frac{Gm(r)}{r} dm. \quad (2.2.8)$$

On integrating the left side of equation (2.2.7) by parts, we get

$$E_{gr} = P(r)4\pi r^3|_0^R - 3 \int_0^R (4\pi r^2)P(r)dr. \quad (2.2.9)$$

Here, the first term in the above equation becomes zero, considering pressure outside $r = R$ and volume at the center are zero. For the second term on integration becomes

$$E_{gr} = -3\bar{P}V, \quad (2.2.10)$$

$$- \int_{m=0}^{m=M} \frac{Gm(r)}{r} dm = -3\bar{P}V, \quad (2.2.11)$$

$$-\frac{1}{3} \frac{E_{gr}}{V} = \bar{P}. \quad (2.2.12)$$

This is first form of the *virial theorem*, the average internal pressure is one third of the density of the stored gravitational energy. Now, from the perfect gas law we have $PV = NkT$ and $E_{th}=3/2 PV$, if the pressure is averaged over volume and integrated we get

$$E_{th} = \frac{3}{2}\bar{P}V, \quad (2.2.13)$$

and we finally get the second form of *virial theorem*

$$E_{th} = \frac{1}{2}(-E_{gr}), \quad (2.2.14)$$

which explains that with the decrease of gravitational energy thermal energy rises (as the star collapse its gravitational self energy becomes more negative, its thermal energy rises). Now total energy becomes

$$E_{tot} = E_{gr} + E_{th} = -E_{th}, \quad (2.2.15)$$

This shows that, the total energy of the star composed of a classical, non-relativistic ideal gas is negative, which explains that the star is bound.

2.3 Energy Transport

In order for the stars to shine the conditions of radiation, conduction and convection must be known. The process of conduction occurs in solids and as stars are not in the form of solid we are not going to discuss conduction here. There are two cases for energy transport [11]. *Radiative* energy transport and the *convective* energy transport.

Radiative Equilibrium

Equations (2.2.8), (2.2.11) and the EoS, $P = P(\rho, T)$, constitute three equations for five variables $P(r), \rho(r), M(r)$, and $T(r)$. The equation for the variation of temperature with radial distance is now required. It depends upon the physical processes that are operating in the particular region of the star [9]. If the energy generated in the nuclear processes, or any other reactions, is transported outwards, then we can relate the energy flux to the temperature gradient, using equation (2.2.6)

$$F(r) = \frac{L(r)}{4\pi r^2} = \frac{-4acT^3}{3\rho\kappa} \left(\frac{dT}{dr} \right), \quad (2.3.1)$$

where $L(r)$ is the luminosity, $F(r)$ is the energy flux. The quantity κ is the radiative opacity of the star. It is a function of T and ρ , i.e., $\kappa = \kappa(\rho, T)$. The above relation says that if the radiative energy flux is F , then the corresponding momentum flux is F/c . If the scattering cross-section is σ and the number density of scatterers is n , then the momentum scattered per second per unit volume will be, $(n\sigma/c)F = (\rho\kappa/c)F$. This quantity is force per unit volume and hence should be equal to $-\alpha P_{rad} = (4aT^3/3)\alpha T$. Thus, equating these two will allow us to give the expression of radiative flux F in terms of temperature gradient. The above expression can be inverted to find the temperature variation that is due to the radiative flux.

$$\frac{dT}{dr} = -\frac{3}{4ac} \frac{\kappa\rho}{T^3} \frac{L_r}{4\pi r^2}. \quad (2.3.2)$$

Opacity

It depends upon the densities, temperatures and element abundance or composition. These are three main sources of opacity. Bound-bound, bound-free (photo-ionization) and free-free absorption (bremsstrahlung).

Bound-Bound Opacity In a bound-bound opacity, an ion or atom is excited to a higher energy level, by the absorption of a photon. Thus, κ is small for all the wavelengths except those where the wavelength corresponds to the energy difference between two atomic levels. The scattering of photons by free electrons corresponds to the electron-scattering opacity.

$$\kappa_{es} = 0.2(1 + X)cm^2g^{-1}, \quad (2.3.3)$$

where X is the mass fraction of hydrogen. The constant value (0.2) comes from the Thomson cross-section σ_T multiplied by n_e , the number of electrons and divided by the electron density ρ .

Free-Free Absorption It is the inverse process of free-free emission that is also known as bremsstrahlung (braking radiation). In a free-free emission, through the electrical potential of an ion, a free electron is accelerated, and as a result, it radiates. Inversely, in free-free absorption, a photon is absorbed by a free electron and an ion, which shares the photon momentum and energy. The free-free absorption contributes an opacity that is given as

$$\kappa_{ff} = 4 \times 10^{22}(X + Y)(1 + X)\rho T^{-3.5}cm^2g^{-1}, \quad (2.3.4)$$

where Y is the mass fraction of helium and Z is the mass fraction of all elements heavier than hydrogen.

Bound-Free Opacity This is a familiar process of photo-ionization, which will occur for all photon energies as long as $h\nu$ is greater than the ionization potential

of a given atomic energy level. So, the ionization of atoms leads to the bound-free opacity, it has the form

$$\kappa_{bf} = 4 \times 10^{25} Z(1 + X) \rho T^{-3.5} \text{cm}^2 \text{g}^{-1}. \quad (2.3.5)$$

Both the bound-free and free-free follows the Kramer's rule where the function is directly proportional to $T^{-3.5}$.

Convective Equilibrium

Energy transport might be due to convection rather than radiative transport, in some regions of the star. Convection occurs when the volume element of material that is displaced from its equilibrium position, rather than returning to the original position, starts moving in the direction of displacement. To see the conditions for the convection to occur, let us consider a volume element of gas at equilibrium radius r inside a star, where the temperature, density, and pressure are T , ρ and P , respectively [10].

Now, make a small displacement of the element to a new radius $r + dr$, where the parameters of the surroundings are $T + dT$, $P + dP$ and $\rho + d\rho$. Since the gas in the star obeys the ideal gas equations

$$\rho \propto \frac{P}{T}, \quad (2.3.6)$$

the logarithmic derivatives give

$$\frac{d\rho}{\rho} = \frac{dP}{P} - \frac{dT}{T}. \quad (2.3.7)$$

Now, in order to simplify the equation, we will consider that after the displacement, the volume element expands adiabatically, without the exchange of heat with new surroundings (i.e. $dQ = 0$ and the entropy $dS = dQ/T$, is a constant). The element expands until its pressure becomes equal to the pressure of the surroundings and reaches the new parameters $T + \delta T$, $\rho + \delta\rho$, and $P + \delta P = P + dP$. Here, the small changes are identified by δ . The expansion of the element is approximated to be

adiabatic. It obeys the equation of state

$$P \propto \rho^\gamma, \quad (2.3.8)$$

where γ is the adiabatic index, it is the ratio of the heat capacities at constant volume and pressure. The logarithmic derivative gives,

$$\frac{\delta\rho}{\rho} = \frac{1}{\gamma} \frac{\delta P}{P}. \quad (2.3.9)$$

If after the expansion the density is lower than the surroundings, then the element will continue to float up, rather than going back to equilibrium, i.e.

$$\rho + \delta\rho < \rho + d\rho, \quad (2.3.10)$$

or

$$\delta\rho < d\rho. \quad (2.3.11)$$

Dividing both sides by ρ

$$\frac{\delta\rho}{\rho} < \frac{d\rho}{\rho}, \quad (2.3.12)$$

and substituting from equations (2.3.7) and (2.3.9), the condition for convection becomes

$$\frac{1}{\gamma} \frac{\delta P}{P} < \frac{dP}{P} - \frac{dT}{T}, \quad (2.3.13)$$

as $\delta P = dP$,

$$\frac{dT}{T} < \frac{\gamma - 1}{\gamma} \frac{dP}{P}, \quad (2.3.14)$$

dividing by dr , we get

$$\frac{dT}{dr} < \frac{\gamma - 1}{\gamma} \frac{T}{P} \frac{dP}{dr}. \quad (2.3.15)$$

The radial temperature and pressure gradients are both negative, so the condition for convection is that the temperature must decrease with the increasing radius

$$\left| \frac{dT}{dr} \right| > \frac{\gamma - 1}{\gamma} \frac{T}{P} \left| \frac{dP}{dr} \right|. \quad (2.3.16)$$

So, if there is convective equilibrium then,

$$\frac{dT(r)}{dr} = -\frac{\gamma - 1}{\gamma} \frac{T(r)}{P(r)} \frac{Gm(r)\rho(r)}{r^2}. \quad (2.3.17)$$

Convective Instability

The fluid will be unstable to convection if the temperature gradient is too steep.

The criteria for convective instability can be expressed as $\phi > \phi_{ad}$ [9], where

$$\phi \equiv \frac{d \ln T}{d \ln P}, \quad \phi_{ad} \equiv \left(1 - \frac{1}{\gamma}\right). \quad (2.3.18)$$

If the gradient ϕ_{rad} arising due to the radiative transfer is less than ϕ_{ad} , then the fluid is stable under convection, but if ϕ_{rad} is greater than the ϕ_{ad} then we have to take the energy transported due to convection and this is complicated, let us understand this by approximating the situation. In such a case, the gradient will tend to the adiabatic value, $\phi = \phi_{ad}$

$$\phi = \frac{d \ln T}{d \ln P} \left(\frac{dT/dr}{dP/dr} \right) = \phi_{ad}, \quad (2.3.19)$$

now, the equation becomes

$$\frac{dT}{dr} = -\phi_{ad} \left(\frac{Gm}{r^2} \right) \left(\frac{\rho T}{P} \right). \quad (2.3.20)$$

Putting together both the radiative and convective transfers of energy, temperature gradient can be written as [9]

$$\frac{dT}{dr} = \begin{cases} -\frac{3\kappa}{4ac} \left(\frac{\rho}{T^3} \right) \left[\frac{L(r)}{4\pi r^2} \right], & \text{if } \phi_{rad} \leq \phi_{ad} \\ -\phi_{ad} \left(\frac{Gm}{r^2} \right) \left(\frac{\rho T}{P} \right), & \text{if } \phi_{rad}(r) \geq \phi_{ad} \end{cases}. \quad (2.3.21)$$

2.4 Equation of Thermal Equilibrium

The energy produced within the shell and the increase in the luminosity of the star as we move from inside towards outside are in direct proportion. Let $L(r)$ be the energy flow across the sphere with radius r , then the net energy loss in the shell from r to $r + dr$ is

$$L(r + dr) - L(r) = \frac{dL(r)}{dr} dr. \quad (2.4.1)$$

If $\epsilon(r)$ is the energy produced per unit mass in unit time, the total energy produced in the shell is

$$\epsilon(r) dm = \epsilon(r) \rho(r) 4\pi r^2 dr. \quad (2.4.2)$$

For the star to be in thermal equilibrium, the radiation loss in the star must be equal to the energy gain from the nuclear burning

$$\frac{dL(r)}{dr} dr = 4\pi r^2 \rho(r) \epsilon(r) dr, \quad (2.4.3)$$

or

$$\frac{dL(r)}{dr} = 4\pi r^2 \rho(r) \epsilon(r), \quad (2.4.4)$$

which is the equation of energy conservation.

2.4.1 Gravitational Instability and Mass Scales

In this section, the conditions will be discussed under which an interstellar gas cloud can collapse. This criterion was presented by a British scientist Sir James Hopwood Jeans (1877-1946).

Jeans' Mass

When a star collapses under self-gravity, it releases the gravitational potential energy. If this energy got trapped inside the core it will increase the thermal energy of the star. This would, in turn, trigger nuclear reactions inside the core due to an increased temperature, as explained in the previous chapter. The contraction of the core starts due to the triggered nuclear reactions and will result in the expansion of the outer layers of the star, forming a gaseous envelope around the star. Let us consider the cloud of pure molecular hydrogen (PMH). For the gravitational collapse to occur, this cloud should fulfill the Jeans' criteria. The Virial theorem (2.2.14) can be written as

$$2K + \Omega = 0, \quad (2.4.5)$$

the kinetic energy is the result of the motion of particles of the cloud. So, if the total number of molecules is N_H , the kinetic energy from the ideal gas equation is

$$K = \frac{3}{2} N_H k T. \quad (2.4.6)$$

Now, finding the gravitational potential energy. Let us assume that the cloud is spherically symmetric with a radius r . The mass enclosed by the cloud is M and has a uniform mass density ρ and temperature T . As the cloud collapses under gravity, there will be a change in mass

$$dm = 4\pi r^2 \rho(r) dr, \quad (2.4.7)$$

so,

$$m(r) = \int_0^r 4\pi r^2 \rho(r) dr. \quad (2.4.8)$$

If we assume a constant density, the gravitational potential energy becomes

$$d\Omega = -\frac{G(4\pi r^2 \rho dr)m(r)}{r}, \quad (2.4.9)$$

then, integrating it with limits for radius is 0 to R , we obtain

$$\Omega = -\frac{16}{15}\pi^2 \rho^2 R^5. \quad (2.4.10)$$

From volume $V = 4/3\pi R^3$ we get the value of density. Now, eliminating the density from equation (2.4.10)

$$\Omega = -\frac{3}{5}\frac{GM^2}{R}. \quad (2.4.11)$$

Now, putting this in equation (2.4.5) we get

$$5N_H kT = \frac{GM^2}{R}. \quad (2.4.12)$$

There might be three cases; first, when in equation (2.4.5), the equality holds and the system is in virial equilibrium. The second possibility, might be the increased kinetic energy as compared to the gravitational potential energy, (i.e. $K > \Omega$, there will be expansion. The gravitational instability is achieved when the change in the gravitational potential energy is greater than the rise in the thermal energy [10]. The collapse occur if the kinetic energy is less than the potential energy ($K < \Omega$). For this case, (the virial theorem) equation (2.4.5) becomes

$$5N_H kT < \frac{GM^2}{R}. \quad (2.4.13)$$

Or

$$M > \frac{5RkT}{m_H}. \quad (2.4.14)$$

We can get the radius R from the volume $V = 4/3\pi R^3$ and then, put it in equation (2.4.14) we get

$$M > \left(\frac{5kT}{Gm_H} \right)^{3/2} \left(\frac{4}{3\rho\pi} \right)^{1/2}. \quad (2.4.15)$$

The mass of the cloud should be greater than the Jeans' mass, so

$$M > M_J, \quad (2.4.16)$$

where M_J is

$$M_J = \left(\frac{5kT}{Gm_H} \right)^{3/2} \left(\frac{3}{4\pi\rho} \right)^{1/2}. \quad (2.4.17)$$

Jeans' Radius

The mass of the cloud is given by the equation

$$M = \frac{4}{3}\rho\pi R_c^3, \quad (2.4.18)$$

where R_c is the radius of the cloud. Putting this value of mass in equation (2.4.14), we get

$$R_c > \left(\frac{15}{4} \frac{kT}{G\pi m_H \rho} \right). \quad (2.4.19)$$

So, Jeans' radius is

$$R_J = \left(\frac{5}{14} \frac{kT}{G\rho\pi m_H} \right). \quad (2.4.20)$$

This relation is called the Jeans' length or the Jeans' radius. The Jeans' density can be written as

$$\rho_J = \left(\frac{3}{4\pi M^2} \right) \left(\frac{5kT}{Gm_H} \right)^3, \quad (2.4.21)$$

which is obtained by the equation (2.4.17).

2.5 Free-Fall Time

In this section, we will discuss the timescale of the molecular cloud collapse. It is also known as the free-fall time. The time a cloud would take to collapse from its original shape to a single point due to the gravitational pull, neglecting the gas pressure that would counteract this gravitational collapse. Consider a small mass m at the surface R of a spherical cloud of mass M . The mass m is initially at rest but it comes inward with following the surface as the surface contracts under gravity. Under the free-fall assumption, when the surface contracts from R to r , the kinetic energy is equal to the difference of the gravitational potential energies between the final and the initial positions.

$$K.E = \frac{1}{2}mv^2 = \frac{1}{2}m\frac{dr^2}{dt} = \frac{GMm}{r} - \frac{GMm}{R}. \quad (2.5.1)$$

The velocity of the particle can be expressed as

$$\frac{dr}{dt} = -\left(\frac{2GM}{R} - \frac{2GM}{r}\right)^{\frac{1}{2}}. \quad (2.5.2)$$

The time variable here, can be isolated upon integration

$$t_{ff} = \int_R^0 \left(\frac{2GM}{R} - \frac{2GM}{r}\right)^{-\frac{1}{2}} dr. \quad (2.5.3)$$

This integral is solved by performing the change of variable $x = r/R$,

$$t_{ff} = \left(\frac{R^3}{2GM}\right)^{\frac{1}{2}} \int_0^1 \left(\frac{x}{1-x}\right)^{\frac{1}{2}} dx, \quad (2.5.4)$$

and here we have a definite integral which is equal to $\pi/2$, t_{ff} becomes

$$t_{ff} = \frac{\pi}{2} \left(\frac{R^3}{2GM}\right)^{\frac{1}{2}}. \quad (2.5.5)$$

Now, by putting $M = \frac{4}{3}\pi R^3\rho$ we get

$$t_{ff} = \frac{\pi}{2} \left(\frac{3}{8\rho G}\right)^{\frac{1}{2}}, \quad (2.5.6)$$

or

$$t_{ff} = \left(\frac{3\pi}{32\rho G} \right). \quad (2.5.7)$$

The free-fall time is much smaller than the time for the evolution of main sequence stars.

2.6 Scaling Relations on the Main Sequence

The observed functional forms (for the main sequence stars) of mass-luminosity relation, $L \sim M^\alpha$ and temperature-luminosity relation, $L \sim T_{eff}^8$ can be explained by the stellar equations deduced above. Assume that the functions $P(r)$, $M(r)$, $\rho(r)$ and $T(r)$ are the roughly the power laws, i.e. $P(r) \sim r^\beta$, and $M(r) \sim r^\alpha$, etc. If we write first three differential equations as scaling relations then,

$$P \sim \frac{M\rho}{r}, \quad (2.6.1)$$

$$M \sim r^3 \rho, \quad (2.6.2)$$

$$L \sim \frac{T^4 r}{\rho \kappa}. \quad (2.6.3)$$

For the moderately massive stars, the pressure will be dominated by the kinetic gas pressure and opacity by the electron scattering.

$$P \sim \rho T. \quad (2.6.4)$$

κ_{es} becomes constant. Now equating (2.6.1) and (2.6.4) we find

$$T \sim \frac{M}{r}, \quad (2.6.5)$$

substituting (2.6.5) into (2.6.3) to express ρr^3 we find

$$L \sim M^3, \quad (2.6.6)$$

as observed for the main sequence stars. The equation (2.6.5) also suggests that $r \sim M$. In order to see this let us consider a star contracting under its own gravity and heating up. This contraction will stop when the high density and temperature

will start the nuclear reactions and the star would stop contracting because of the equilibrium. For any mass M , the star will stop shrinking when the core temperature reaches to the critical temperature i.e. \bar{T} . This is because of the dependence of nuclear power density on temperature. By using $r \sim M$, we see from equation (2.6.2)

$$\rho \sim M^{-2}. \quad (2.6.7)$$

This shows that the more massive stars will have lower density and low mass stars will have high density, as the density decrease with an increase in M^{-2} . In the low mass stars, high density signifies the dominant role of bound-free and free-free opacity.

$$\kappa \sim \frac{\rho}{T^{3.5}}, \quad (2.6.8)$$

Since $T \sim \text{constant}$, $r \sim M$ and $\rho \sim M^{-2}$ then $\kappa \sim \rho \sim M^{-2}$ and the equation (2.6.3) gives

$$L \sim \frac{T^4 r}{\kappa \rho} \sim \frac{r}{\rho^2} \sim M^5, \quad (2.6.9)$$

we get $L \sim M^5$, as seen in the low mass stars. For the most massive stars, due to low density the radiation pressure becomes dominant, and we find

$$P \sim T^4, \quad (2.6.10)$$

and electron scattering with $\kappa_{es} = \text{constant}$, will become the source of opacity. We find $L \sim M$, by substituting equation (2.6.10) in equation (2.6.3) and then equating the result with (2.6.1). This relation $L \sim M$ holds for the most massive stars. The functional dependence of the main sequence stars in the HR diagram can be reproduced. We found $L \sim M^3$ for the moderately mass stars and $L \sim M^5$ for the low mass stars. Let us see by taking an intermediate slope say $L \sim M^4$ and since $r \sim M$ then equation (1.2.4) becomes

$$\sigma T_{eff}^4 = \frac{L}{4\pi r^2} \sim \frac{M^4}{M^2} \sim M^2 \sim L^{\frac{1}{2}}, \quad (2.6.11)$$

so

$$L \sim T_{eff}^8, \quad (2.6.12)$$

as observed. The mass-luminosity and the surface-temperature-luminosity relations of the main sequence stars are the consequences of different sources of pressure and opacity for the different masses of stars and also the fact that hydrogen burning keeps the core temperatures of all the main sequence stars in a narrow range.

2.7 The Equation of State (EoS)

To determine the equilibrium structure of stars we can integrate the given functions $P(\rho, T)$, $\kappa(\rho, T)$ and $\epsilon(\rho, T)$, if the boundary conditions are known. Here, $P(\rho, T)$ is usually called the equation of state [10]. Where we required P and ρ to vanish at a point $r = R$. $M(r)$ and $L(r)$ approaches to zero as $r \rightarrow 0$.

$$M(r = 0) = 0, L(r = 0) = 0, P(r = r_*) = 0, M(r = r_*) = M_*, \quad (2.7.1)$$

where M_* is the total mass of the star. Now we can rewrite the equations of stellar structure with M_r as an independent variable and to treat $r = r(M_r)$ as a dependent function. The corresponding equations can be written by dividing the equations of stellar structure by equation (2.2.3). We have ended up with seven coupled equations that are defining the seven unknown functions: $M(r)$, $L(r)$, $\rho(r)$, $P(r)$, $T(r)$, $\kappa(r)$ and $\epsilon(r)$. As there are four boundary conditions for the four first-order differential conditions so if there is a solution, it will be unique. Now we get,

$$\frac{dP}{dM_r} = -\frac{GM(r)}{4\pi r^4}, \quad (2.7.2)$$

$$\frac{dT}{dP} = -\frac{\phi_{ad}}{4\pi} \left(\frac{T}{P} \right) \left(\frac{GM(r)}{r^4} \right), \quad (2.7.3)$$

$$\frac{dT}{dP} = -\frac{3\kappa}{64acT^3} \frac{L(r)}{\pi^2 r^4}, \quad (2.7.4)$$

$$\frac{dL(r)}{dM(r)} = \epsilon, \quad (2.7.5)$$

$$\frac{dr}{dM(r)} = \frac{1}{4\pi r^2 \rho}. \quad (2.7.6)$$

If the mass of the star is taken to be M , then boundary conditions become, at the center ($M_r = 0$), $r = L_r = 0$, at the surface ($M_r = M$), $\rho = T = 0$.

At the origin the boundary conditions are obvious but at the surface, we have to use some approximation. At the stellar surface, if the temperature T is zero then no radiations come out of the star. So, under such complications, the boundary conditions provided above do serve well, as long as the resulting solution is used in the interior of the star.

2.7.1 The Ideal Gas

Consider a gas such that it is a mixture of three different kinds of particles, with masses m_1, m_2 and m_3 and densities n_1, n_2 and n_3 . The mean particle mass will be

$$\bar{m} = \frac{n_1 m_1 + n_2 m_2 + n_3 m_3}{n_1 + n_2 + n_3} = \frac{\sum_i n_i m_i}{\sum_i n_i} = \frac{\rho}{n}. \quad (2.7.7)$$

The mean mass depends on the chemical abundance and the ionization state of the gas. The gaseous pressure P_g will be

$$P_g = nkT = \frac{\rho}{\bar{m}} kT. \quad (2.7.8)$$

Now, for a completely ionized pure hydrogen the mean mass is $\bar{m} = m_H/2$. The number densities of hydrogen and helium will be

$$n_H = \frac{X\rho}{m_H}, n_{He} = \frac{Y\rho}{4m_H}. \quad (2.7.9)$$

Similarly, for an element of mass number A (i.e. an element with a total number of A protons and neutrons in each atomic nucleus)

$$n_A = \frac{Z_A \rho}{A m_H}, \quad (2.7.10)$$

where Z_A is the mass abundance of an element of atomic mass number A . The ionization of hydrogen results in two particles, of helium, three particles and of atom with atomic number Z , results in $Z + 1$ particles (which is close to $A/2$, for heavy particles). so for a completely ionized gas the total number density will be

$$n = 2n_H + 3n_{He} + \sum \frac{A}{2} n_A, \quad (2.7.11)$$

putting the values of number densities and using $X + Y + Z = 1$ which is used for the mass fraction of metals [10]

$$n = \frac{\rho}{m_H} \left(2X + \frac{3}{4}Y + \frac{1}{2}Z \right), \quad (2.7.12)$$

$$n = \frac{\rho}{2m_H} \left(3X + \frac{Y}{2} + 1 \right). \quad (2.7.13)$$

2.8 Polytropic Models for Stars

Consider a spherically symmetric star in hydrostatic equilibrium. The two ordinary, first order differential equations of hydrostatic equilibrium (2.2.6) and the continuity equation (2.7.6) are combined. Then, eliminating $M(r)$, we get

$$r^2 \frac{d}{dr} \left(\frac{1}{\rho} \frac{dp}{dr} \right) + \frac{2r}{\rho} \frac{dP}{dr} = -4\pi G \rho r^2. \quad (2.8.1)$$

Now, combining the terms on the left side of the equation we get

$$\frac{d}{dr} \left\{ \frac{r^2}{\rho} \frac{dP}{dr} \right\} = -4\pi G r^2 \rho. \quad (2.8.2)$$

For the stars in convective equilibrium we get a relation between the two unknowns pressure and density i.e. $P(r)$ and $\rho(r)$. Putting these in an adiabatic relation equation (2.3.8) $P \propto \rho^\gamma$ or

$$P \propto \rho^{1+\frac{1}{n}}, \quad (2.8.3)$$

where $\gamma = \frac{C_p}{C_v}$, where C_p and C_v are the specific heats at constant pressure and constant volume, respectively. Such configurations are called *polytropes*, and $n = \frac{1}{\gamma - 1}$ is called the *polytropic index* [11]. Polytropes are given by the EoS in which pressure is expressed as a power law in density, Now, converting proportionality into equality in equation (2.3.8) and equation (2.8.3) we have,

$$P = \kappa \rho^\gamma, \quad (2.8.4)$$

$$P = \kappa \rho^{1+\frac{1}{n}}. \quad (2.8.5)$$

For the polytropic EoS we substitute

$$\rho = \rho_c \theta^n, \quad (2.8.6)$$

so that the pressure P becomes

$$P = \kappa \rho_c^{1+\frac{1}{n}} \theta^{1+\frac{1}{n}}. \quad (2.8.7)$$

Now, putting the values of equation (2.8.6) and equation (2.8.7) in equation (2.8.2), we get

$$\frac{1}{r^2} \frac{d}{dr} \left(r^2 \kappa \rho_c^{\frac{1}{n}} (1+n) \frac{d\theta}{dr} \right) = -4\pi G \rho_c \theta^n, \quad (2.8.8)$$

substituting $r = \alpha \xi$, where ξ is a dimensionless variable, above equation becomes

$$\frac{1}{4\pi G \alpha^2 \xi^2} \frac{d}{d\xi} \left(\xi^2 \kappa \rho_c^{\frac{1}{n}-1} (1+n) \frac{d\theta}{d\xi} \right) = -\theta^n. \quad (2.8.9)$$

The constant α becomes

$$\alpha^2 = \frac{\kappa (1+n) \rho_c^{\frac{1}{n}-1}}{4\pi G}. \quad (2.8.10)$$

After substituting the value of α in equation (2.8.9)

$$\frac{1}{\alpha^2 \xi^2} \frac{d}{d\xi} \left(\xi^2 \alpha^2 \frac{d\theta}{d\xi} \right) = \theta^n. \quad (2.8.11)$$

$$\frac{1}{\xi^2} \frac{d}{dr} \left(\xi^2 \frac{d\theta}{d\xi} \right) + \theta^n = 0. \quad (2.8.12)$$

This is the dimensionless form of the equation (2.8.2) For n the polytropic index, this final equation is the *Lane-Emden* equation [14, 15]. If $\gamma = \infty$ then $n = 0$, we have $\rho \propto P^0 = \text{constant}$, the star is in a uniform density. If $\gamma = 5/3$, which is the value of the ratio of specific heat constants, we have $n = 3/2$, the star is in convective equilibrium. If $n = 3$ we have $\gamma = 4/3$, which is the ultra-relativistic case. For, $n=\infty$, $\gamma = 1$ the star is in an isothermal configuration [14, 15].

Chapter 3

Compact Stars

There are stars whose dynamics is unexplainable from the classical physics, the reason being their higher mass than expected. These stars make up a special class of compact stars. If these compact stars were formed by collapsing stars, they must have had transformed into black holes.

If a normal neutron star or white dwarf gains mass by accretion from the surrounding disc of matter, the centrifugal force would resist the gain. Abramowicz [16], while studying the centrifugal force in general relativity (GR), found that near a black hole the centrifugal force reverses the direction thus, the gain in mass is not opposed by the centrifugal force.

Unlike normal stars, compact stars do not produce energy by annihilation and so, if they are massive enough, should undergo continuous collapse. The degeneracy pressure of electrons or neutrons, stops further collapse. In this chapter, we study the physics required for understanding the neutron stars, learning the study of GR and Abramowicz's analysis of the centrifugal force for Chapter 4. We will not pursue the application of the centrifugal force stabilizing the neutron stars, which was undertaken by Freire and Costa [17] and later by Abramowicz and Lasota [18].

3.1 Degenerate Fermi Gas of Electrons

In classical mechanics, the states of the free particles have a continuous energy spectrum and there is no limit on the number of particles that can be found in these continuous states. When the energy level corresponds to more than one independent quantum state, that energy level is said to be degenerate.

Maxwell, through the kinetic theory of gases, by considering the kinetic energy of random motion of particles, was able to find the internal energy, temperature, pressure, etc that are included in the standard formalism of classical thermodynamics. However, when it comes to temperature and entropy, the former is directly measurable but the entropy is not. The formalism followed by Maxwell only includes velocities of particles, which was basically inspired from Newtonian and Lagrangian mechanics. Boltzmann, on the other hand, followed the Hamiltonian way, which relies on a $6N$ dimensional phase-space, that is the positional space and the momentum space together. A particular microstate of a system (a gas of N particles) can be specified through $6N$ position and momentum coordinates. A system whose Hamiltonian function $H(q, p)$ is a constant, makes an *isolated* system [19].

An ensemble represents the thermodynamic state of a system. If the distribution function, $f(q, p)$, is zero everywhere except the points where $H(q, p) = E$, is a constant, the corresponding ensemble is called the *microcanonical ensemble*. For a mechanical system, which has an exactly specified energy, the microcanonical ensemble represents its possible states. In this system no exchange of energy and number of particles is allowed as the total energy is conserved. Since $E = p^2/2m$ for zero potential, we only allow collisions that collectively leave the total momentum squared of the colliding particles the same.

If we have a distribution function f , with all its possible states e.g, from 1 to ν , we must have

$$\sum_{i=1}^{\nu} f_i = 1. \tag{3.1.1}$$

The canonical ensemble is a collection of systems, all at same temperature. We can say that if the distribution function, f , in phase-space, is proportional

to $\exp[-H(q, p) / kT]$, this ensemble is called the *canonical ensemble* [19]. So, we have another constraint along with equation (3.1.1)

$$\Sigma_i f_i = 1 ; \Sigma_i f_i E_i = U, \quad (3.1.2)$$

where i is the different modes of distribution and U is the total energy.

Consider we have n_1 indistinguishable particles of one type, n_2 of another, ..., n_ν of some other. So, these particles, distributed among ν different modes with energy E_ν , can be written as

$$N = n_1 + n_2 + \dots n_\nu = \Sigma_{i=1}^\nu n_i. \quad (3.1.3)$$

If the chemical reactions are allowed, then we may have an increase or a decrease in the number of particles. In this case, the energy associated with changing number of particles is μdN where μ is the chemical potential. The number of particles will be varying through number density from point to point and if the average is taken over all, the average number density will remain constant.

The grand canonical ensemble assigns a probability to each distinct microstate $f = \exp[\Omega + \mu N + E/kT]$. Here, Ω is the grand potential and is constant for the ensemble, μ is the chemical potential and E is the total energy of a microstate. So, we can say that the grand canonical ensemble is used to represent the possible microstates of a mechanical system of particles in thermodynamic equilibrium (both thermal and chemical). Only the average energy U and the averaged number of particles \bar{N} (averaged over the ensemble), will be specified. So, now we have the *grand canonical ensemble*, with another constraint, including equation (3.1.2) as

$$\Sigma_{N,i} f_{N,i} = 1, \quad (3.1.4)$$

$$\Sigma_{N,i} E_{N,i} f_{N,i} = U, \quad (3.1.5)$$

$$\Sigma_{N,i} N_i f_{N,i} = \bar{N}. \quad (3.1.6)$$

In the context of basic units of phase-space, we can find the number of possible states, for a given energy and then it can be written as

$$S = -k_B \Sigma_{N,i} f_{N,i} \ln(f_{N,i}); \quad \Sigma_{N,i} f_{N,i} = 1, \quad (3.1.7)$$

where k_B is the Boltzmann constant. Here, U , S and \bar{N} are related to the usual thermodynamic relations $U = TS + \Omega + \bar{N}\mu$ and Ω is the grand canonical function. However, the electrons that are the indistinguishable identical particles, if we take these identical particles and interchange them, it will make no difference to the wave-function.

Consider the wave-function of a system of two identical, indistinguishable, quantum mechanical particles. In one spatial dimension, the wave-function of a two-particle system is a function of two variables x_1 and x_2 . So, the system is such that interchanging the particles, the probability density $|\Psi|^2$ of the system must not change [20].

$$|\Psi(x_1, x_2)|^2 = |\Psi(x_2, x_1)|^2, \quad (3.1.8)$$

$$\Psi(x_1, x_2) = \pm \Psi(x_2, x_1). \quad (3.1.9)$$

The wave functions go with the positive or negative signs, or they are either even or odd. The total wave-function is antisymmetric when (3.1.9) is negative whereas it is symmetric when (3.1.9) is positive. Particles of the former type (antisymmetric wave-function) are called fermions and of the latter type (symmetric wave-function), bosons. Since the change of a function to its negative is to give the same answer, the wave-function for a pair of fermions in the same state must be zero, so they obey Pauli exclusion principle. Solving the Dirac equation, the fermions must have spin of an odd multiple of $\hbar/2$. Those of the bosons are multiples of \hbar ¹.

Bosons can occupy single state at low temperature and become Bose-Einstein condensate but electrons become a degenerate Fermi gas, because only the lowest states are occupied, and the states have to be all distinct. The total minimum energy of the lowest occupied states is the Fermi Energy, with a corresponding Fermi momentum.

Now, consider the six dimensional phase-space, consisting of three spatial and

¹Using quantum field theory, it can be shown that half integer spin particles will follow Fermi-Dirac statistics while integer spin particles will follow Bose-Einstein statistics.

three momentum components; then

$$d^3x d^3p \sim \hbar^3. \quad (3.1.10)$$

The volume in spherical coordinates is

$$\Delta p_x \Delta p_y \Delta p_z = 4\pi p^2 \Delta p = 4\pi m_e^3 V^2 \Delta V, \quad (3.1.11)$$

where classical physics is assumed to be valid for the momentum of free electrons ($p = m_e V$). In terms of the momentum, we state the average kinetic energy and pressure in case of non-relativistic gas [4].

$$P_e = \frac{2}{3} n_e E_{avg} = \frac{2}{3} n_e \left(\frac{p^2}{2m_e} \right)_{avg}, \quad (3.1.12)$$

the subscript 'e' is used for the electron degeneracy pressure, which is the primary source of degenerate pressure in white dwarf stars. The volume of the shell in phase-space at a momentum p in the physical volume is $4\pi p^2 V dp$. Dividing the electron number N_e to obtain the fraction of electrons in the shell and $p = |\mathbf{p}|$. From equation (3.1.10) we have

$$d^3p dV > (\hbar)^3, \quad (3.1.13)$$

which defines the volume of a cell in a six dimensional (position-momentum) phase-space. Now, using the Fermi-Dirac distribution let us calculate the average of $(p^2/2m_e)$ over a momentum distribution. The Fermi-Dirac distribution is [20]

$$dN = \frac{2s+1}{e^{(E-\mu(T))/kT} + 1} \frac{d^3p dV}{(h)^3}, \quad (3.1.14)$$

where s is the spin of particle (each fermion). For degenerate electrons ($s=1/2$ particles), the phase-space distribution is

$$dN(p) dp = \begin{cases} 2 \times 4\pi p^2 \frac{dp dV}{(h)^3}, & \text{if } |p| \leq p_f \\ 0, & \text{if } |p| > p_f \end{cases}, \quad (3.1.15)$$

where p_f is called the Fermi momentum (which is the magnitude of momentum corresponding to Fermi energy E_f). The number density of electrons of a given

momentum from equation (3.1.15) comes out to be

$$n_e(p)dp = \begin{cases} 8\pi p^2 \frac{dp}{(h)^3}, & \text{if } |p| \leq p_f \\ 0, & \text{if } |p| > p_f \end{cases}. \quad (3.1.16)$$

Integrating over all momenta, we will get a relation between Fermi momenta p_f and electron density n_e .

$$n_e = \int_0^{p_f} \frac{8\pi}{(h)^3} p^2 dp = \frac{8\pi}{3(h)^3} p_f^3. \quad (3.1.17)$$

For a non-relativistic degenerate electron gas, we replace $n(p)$ in the given equation

$$P = \frac{1}{3} \int_0^\infty n(p) p v dp, \quad (3.1.18)$$

with Fermi-Dirac distribution in the degenerate limit (3.1.5) and using (3.1.6), where $v = p/m_e$, we get [21]

$$P_e = \frac{1}{3} \int_0^{p_f} \frac{8\pi}{(h)^3} \frac{p^4}{m_e} dp = \left(\frac{3}{8\pi} \right)^{2/3} \frac{(h)^2}{5m_e} n_e^{5/3}. \quad (3.1.19)$$

For a general form, let us consider a fully ionized gas composed of a particular element, of atomic Z and atomic mass A and with the density of ions n_{ion} . Then we have

$$n_e = Z n_{ion} = \left(\frac{Z}{A} \right) \frac{\rho}{m_H}. \quad (3.1.20)$$

Substitute this value of number density of electron in equation (3.1.19) we get

$$P_e = \left(\frac{3}{\pi} \right)^{2/3} \frac{(h)^2}{20m_e m_H^{5/3}} \left(\frac{Z}{A} \right)^{5/3} \rho^{5/3}, \quad (3.1.21)$$

where m_H is the mass of hydrogen atom. This equation is now in the form of the EoS of a *degenerate non-relativistic electron gas*.

Equate (3.1.19) with the equation of central pressure $P_c \approx [\pi/36]^{1/3} GM^{2/3} \rho_c^{4/3}$ [21], then

$$\frac{(h)^2}{5m_e} \left[\frac{3}{8\pi} \right]^{2/3} \left[\frac{X_e \rho_c}{m_H} \right]^{5/3} \approx \left[\frac{\pi}{36} \right]^{1/3} GM^{2/3} \rho_c^{4/3}. \quad (3.1.22)$$

Here, X_e is the number of electrons per nucleon (Z/A). Now, solving the above equation to get the density at the center of a cold (non-relativistic degenerate) white dwarf.

$$\rho_c \approx \frac{3.1}{X_e^5} \frac{m_H}{(h/m_e c)^3} \left[\frac{M}{M_*} \right]^2, \quad (3.1.23)$$

where $M_* \approx \alpha_G^{-3/2} m_H \approx 1.85 M_\odot$ is the stellar mass, [21]. The mass scale of the main sequence stars is determined by this stellar mass. The dimensionless number $\alpha_G = G m_H^2 / \hbar c \approx 5.9 \times 10^{-39}$ measures the strength of the interaction between nucleons. The equation (3.1.23) is obtained by considering that the star is balanced by the pressure of non-relativistic degenerate electron gas. The (electron) gas becomes relativistic when the number density of the electrons is greater as compared with $m_H(m_e c/h)^3$. It follows that the non-relativistic equation (3.1.23) will only be followed if the mass of the white dwarf, M , is small as compared to the M_* . The Fermi momentum p_F and $m_e c$ becomes equal when the electron number density is $8\pi/c(m_e c/h)^3$. The non-relativistic EoS will be allowed, only if the mass of the star M is larger as compared to the mass M_* . The equation (3.1.23) explains that the density will increase with M^2 . This rise occur because at increased densities the electrons become ultra-relativistic. So, the pressure for ultra-relativistic electrons is [21]

$$P = \frac{hc}{4} \left[\frac{3}{8\pi} \right]^{1/3} n_e^{4/3}, \quad (3.1.24)$$

putting the value of the number density of electrons, the pressure due to the ultra-relativistic electrons comes out to be

$$P = \frac{hc}{4} \left[\frac{3}{8\pi} \right]^{1/3} \left[\frac{X_e \rho_c}{m_H} \right]^{4/3}. \quad (3.1.25)$$

Now consider a star of mass M , which is balanced due to the pressure of the ultra-relativistic electrons. The central pressure needed to support the star is [21]

$$P \approx \left[\frac{\pi}{36} \right]^{1/3} G M^{2/3} \rho_c^{4/3}. \quad (3.1.26)$$

By comparing equations (3.1.25) and (3.1.26)

$$\frac{hc}{4} \left[\frac{3}{8\pi} \right]^{1/3} \left[\frac{X_e \rho_c}{m_H} \right]^{4/3} \approx \left[\frac{\pi}{36} \right]^{1/3} G M^{2/3} \rho_c^{4/3}, \quad (3.1.27)$$

we get the mass [21]

$$M = \frac{1}{G} \left[\frac{(h)c}{4} \right]^{3/2} \left[\frac{3}{8\pi} \right]^{1/2} \left[\frac{36}{\pi} \right]^{1/2} \left[\frac{X_e}{m_H} \right]^2. \quad (3.1.28)$$

This is known as the *Chandrasekhar mass*. Now writing in terms of the mass M_* and then in the stellar mass M_\odot , we get the non-relativistic Chandrasekhar mass

$$M_{CH} \approx 2.3X_e^2 M_* \approx 4.3X_e^2 M_\odot. \quad (3.1.29)$$

The Chandrasekhar mass is the limiting mass, for a mass greater than the M_{CH} the degenerate electron gas cannot support a star.

Now considering a model where the relativistic relation between energy and momentum is

$$\epsilon_p^2 = m_e^2 c^4 + p^2 c^2. \quad (3.1.30)$$

Writing equation (3.1.18) as

$$P = \frac{1}{3V} \int_0^{p_F} \frac{p^2 c^2}{\epsilon_p} g(p) dp, \quad (3.1.31)$$

where

$$g(p) dp = \frac{2V}{(h)^3} 4\pi^2 p^2 dp. \quad (3.1.32)$$

Now substitute $x = p/m_e c$ in equation (3.1.31) and inserting the value of Fermi momentum and then the electron number density we also get

$$x_F = \left[\frac{3n_e}{8\pi} \right]^{1/3} \frac{h}{m_e c} = \left[\frac{3X_e \rho_c}{8\pi m_H} \right]^{1/3} \frac{h}{m_e c}. \quad (3.1.33)$$

The substitution gives

$$P = \frac{8\pi m_e^4 c^5}{3(h)^3} \int_0^{x_F} \frac{x^4}{(1+x^2)^{1/2}} dx. \quad (3.1.34)$$

After putting the value of x_F and integrating the equation (3.1.34) we get the pressure of an ideal degenerate electron gas

$$P = \frac{hc}{4} \left[\frac{3}{8\pi} \right]^{1/3} n_e^{4/3} I(x_F), \quad (3.1.35)$$

where

$$I(x) = \frac{3}{2x^4} \left[x(1+x^2)^{1/2} \left(\frac{2x^2}{3} - 1 \right) + \ln[x + (1+x^2)^{1/2}] \right]. \quad (3.1.36)$$

Higher densities give large Fermi momentum $x_F \gg 1$ and equation (3.1.36) tends to 1 and the resulting pressure becomes equal to the pressure of the degenerate ultra-relativistic electron gas [14, 21]. For lower densities, the Fermi momentum is small $x_F \ll 1$ and equation (3.1.36) approaches $4x_F/5$ and the pressure comes out to be equal to the pressure of the non-relativistic electron gas. . Now we compare the pressure (3.1.35) with the hydrostatic pressure required to support the star we have

$$\frac{hc}{4} \left[\frac{3}{8\pi} \right]^{1/3} \left[\frac{X_e \rho_c}{m_H} \right]^{4/3} I(x_F) \approx \left[\frac{\pi}{36} \right]^{1/3} GM^{2/3} \rho_c^{4/3}, \quad (3.1.37)$$

$$\frac{hc}{4} \left[\frac{3}{8\pi} \right]^{1/3} \left[\frac{Y_e}{m_H} \right]^{4/3} \left[\frac{36}{\pi} \right]^{1/3} \frac{1}{G} I(x_F) \approx M^{2/3}, \quad (3.1.38)$$

or

$$M \approx I(x_F)^{3/2} M_{CH}, \quad (3.1.39)$$

where M_{CH} is the Chandrasekhar mass given by equation (3.1.29).

Now, consider the polytropic model of star explained in Section (2.8) for a more accurate result for the Chandrasekhar mass. The relation between pressure and density in the polytropic model equation (2.8.3), and the pressure of the gas for the ultra-relativistic electron gas (3.1.25) are related in a similar manner

$$P(r) \propto \rho(r)^{4/3}. \quad (3.1.40)$$

For $n = 3$, we have $P_c = 0.36GM^{2/3}\rho_c^{4/3}$ [21]. So, the Chandrasekhar mass becomes relativistic [14, 15]

$$M_{CH} = 3.1X_e^2 M_* = 5.8X_e^2 M_\odot, \quad (3.1.41)$$

$$M_{CH} \approx 1.4M_\odot \pm 0.05. \quad (3.1.42)$$

where $X_e \approx 0.5$, when considering two nucleons per electron. The limit for the cold white dwarf is then $0.69 M_\odot$ [10].

3.1.1 The Mass-Radius Relation

According to the relation (3.1.23), the mass density for a white dwarf is an increasing function of its mass. The size of the white dwarf decreases with the increasing mass. To find the mass-radius relation, a model for density distribution is required. The average density of a white dwarf mass M is

$$\langle \rho \rangle \approx \frac{0.51 m_H (m_e c)^3}{X_e^5 (h)^3} \left[\frac{M}{M_*} \right]^2. \quad (3.1.43)$$

If the degenerate electrons were non-relativistic at the start then the stellar structure is approximately same as the polytropic model with polytropic index $n = 3/2$, which gives $P \propto \rho^{5/3}$, and the average density is $\rho/6$ [21]. The mass density relation

$$\rho_c = \frac{M}{\frac{4}{3}\pi R^3}, \quad (3.1.44)$$

is then used to obtain

$$R = \left[\frac{3M}{4\pi \langle \rho \rangle} \right]^{1/3} \approx 0.77 X_e^{5/3} \frac{1}{\sqrt{\alpha_G}} \frac{h}{m_e c} \left[\frac{M_*}{M} \right]^{1/3}. \quad (3.1.45)$$

The Characteristic Size

The constant $\alpha_G \approx 5.9 \times 10^{-39}$ and the Compton wavelength of electron is used to determine the characteristic size of white dwarf. The wavelength is ($h/m_e c = 2.4 \times 10^{-12} m$). The characteristic size is

$$\frac{1}{\sqrt{\alpha_G}} \frac{h}{m_e c} \approx 3 \times 10^7 m, \quad (3.1.46)$$

and the characteristic density is

$$\frac{m_H (m_e c)^3}{(h)^3} \approx 10^8 kg/m^3. \quad (3.1.47)$$

In terms of the solar mass M_\odot and radius R_\odot , and $X_e = 0.5$ we have the mass-radius relation as [15, 21]

$$R \approx \frac{R_\odot}{74} \left[\frac{M_\odot}{M} \right]^{1/3}. \quad (3.1.48)$$

So, the radius of the white dwarf is the decreasing function of its mass.

3.2 The Crab Nebula and Pulsar Detection

At the time of a supernova explosion, section (1.2.6), the nebula formed by the gaseous debris is called the supernova remnant (SNR). A fine example of this is the Crab nebula, or *M1*, which is the nearest supernova remnant [5, 6]. Galelio observed



Figure 3.1: The Crab Nebula seen in the constellation Taurus by the Chinese is the most remarkable event, reported in 1034 A.D. [13].

this nebula through a telescope and drew a picture and noted that it resembled a crab, hence, it was given the name of *Crab Nebula*. It is shown in Figure (3.1). Pulsars are the rotating neutron stars formed from the inner most cores of exploding stars.

The year 1967 marked the discovery of the first pulsar, observed at radio wavelengths on November 28, by Antony Hewish and his student Jocelyn Bell [15, 22, 23]. Hewish won the Nobel Prize of Physics for this discovery of radio pulsar with his colleague Martin Ryle. The star emitted energy in the form of regular pulses i.e. a larger pulse followed by a small [5]. The change in the time rate of pulses (33 milliseconds) was 13.5 microseconds per year [5]. The neutron star present at the center of the Crab Nebula, observed through Suzaku hard R-ray detector can be seen in Fig (3.2).

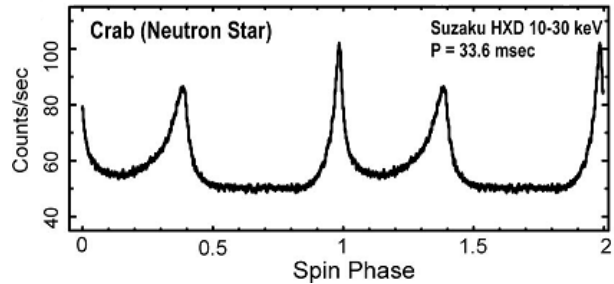


Figure 3.2: The pulses from the center of the Crab Nebula, observed through Suzaku hard R-ray detector (Suzaku HXD) (Courtesy Astrophys.Space Sci.Proc.) .

3.3 Neutron Stars

The identification of pulsars as neutron star was not obvious. Tommy Gold made his first argument, in 1968, about pulsars that they were in fact rapidly rotating neutron stars [5, 24], Figure (3.3). The stability of pulse period was one of the same observed feature in both the neutron stars and pulsars. A few months later, the pulsar NP 0532 [25] was studied, present at the center of the Crab Nebula. Figure (3.2) gives the pulses from the crab nebula observed through Suzaku HXD.

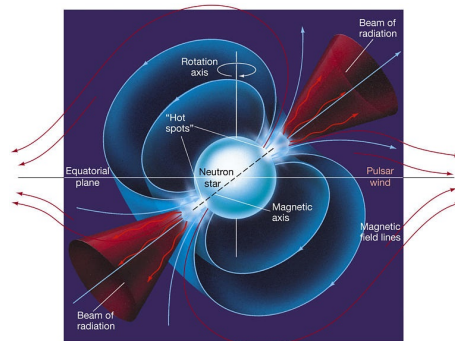


Figure 3.3: The pulsar seen in the figure is the artist's description of the light house model, where the pulsar's beam of light is not aligned with its rotation axis.

For a neutron star its initial core temperature is 10^{11} to $10^{12}K$. This temperature continues to decrease with the emission of neutrinos and it can reduce to a temperature of 10^8K , after some hundred years of its formation. In the periodic table, the most massive nuclei are not stable due to the increased coulomb repulsion, the stars that are less massive are also not stable because of their higher fraction of nucleons near the surface. The most stable nuclei in the periodic table lies near Fe^{56} , because it has the lowest mass per nucleon with binding energy $8.8MeV$ at densities $\sim 10^{14}kgm^{-3}$. At such densities the pressure of relativistic (highly energetic degenerate) electrons can cause inverse beta decay [1, 15]. This is the introduction of neutron stars discussed in Section (1.2.4).

3.3.1 The Size of a Neutron Star

Now, we are going to see how the central density ρ_c and the radius of the star depends upon its mass. In previous section, we assumed that the white dwarf stars are supported by the degenerate electron pressure. Here, we have assumed that the neutron star is held together due to the degenerate neutron pressure. As neutrons are the main constituent here, the number of neutrons n_n is directly determined by the mass density.

$$n_n \approx \frac{\rho_c}{m_n}, \quad (3.3.1)$$

where m_n is the mass of the neutron ($1.6749 \times 10^{-27}kg$). So, $n_n \approx 1.19 \times 10^{44}m^{-3}$. From the corresponding equations for white dwarfs we have for a neutron star

$$P = \frac{(h)^2}{5m_e} \left[\frac{3}{8\pi} \right]^{2/3} n_e^{5/3} = \frac{(h)^2}{5m_e} \left[\frac{3}{8\pi} \right]^{2/3} \left[\frac{X_e \rho_c}{m_H} \right]^{5/3}, \quad (3.3.2)$$

and

$$\rho_c \approx \frac{3.1}{X_e^5} \left[\frac{M}{M_*} \right] m_n \left(\frac{m_n c}{h} \right)^3, \quad (3.3.3)$$

where, $M_* \approx \alpha^{-3/2} m_n = 1.85M_\odot$ is the constant mass. The radius of the neutron star can be found by using the analogy adopted for the white dwarf [21]

$$R_{WD} = \left[\frac{3M}{4\pi < \rho >} \right]^{1/3} \approx 0.77 X_e^{5/3} \left[\frac{M_*}{M} \right]^{1/3} \alpha_G^{-1/2} \frac{h}{m_e c}. \quad (3.3.4)$$

Now, putting $X_e = 1$ for the neutron star we get R_{NS} [21]

$$R = \left[\frac{3M}{4\pi \langle \rho \rangle} \right]^{1/3} \approx 0.77 \left[\frac{M_*}{M} \right]^{1/3} \alpha_G^{-1/2} \frac{h}{m_n c}. \quad (3.3.5)$$

The characteristic size of a neutron star is determined by the strength of gravity, $\alpha_G = 5.9 \times 10^{-39}$ and the Compton wavelength $h/m_n c$ [21], we have

$$\alpha_G^{-1/2} \frac{h}{m_n c} \approx 17 \text{ km}. \quad (3.3.6)$$

In the case of the stellar remnant with mass greater than the mass of the neutron star, there can be two possible cases; either the star undergoes a supernova explosion and becomes a strange star or it collapses into a black hole. To find a lower limit we can use the relation $R \propto M^{-1/3}$. The lower limit would be $\sim 3.6 M_\odot$ [21].

Neutron Drip

Nuclei with lower atomic numbers, when two atoms are closely packed e.g think of two hydrogens that are too close that one of the electron gets merged in the nuclei and inverse beta decay occur, now it is a deuterium ${}_1H^2$. Consider if another hydrogen atom come near this isotope and the same merging and beta decay occur, it will now become the ${}_1H^3$ tritium, with two neutrons and one proton in the nucleus and this is not stable. Similar is the case with heavier nuclei e.g, uranium. ${}_{92}U^{232}$ have isotopes ${}_{92}U^{235}$ and ${}_{92}U^{238}$. Now, if a beta decay occur in ${}_{92}U$ this will decrease its atomic number to ${}_{91}U$, but this will increase the neutrons in the nucleus in an enormous amount. The nucleus will not bear this enormous amount of neutrons and these neutrons will start dripping out of the nucleus.

When nuclei gets squeezed in heavier atoms (having higher number of neutrons), due to the increased densities, inverse beta decay occur, which results in further increase in neutrons. Now, the atomic number becomes lower but the number of electrons increased for the same number of nucleons. The presence of too many neutrons cannot occur in stable atoms. So, when the density of the core exceeds $4 \times 10^{14} \text{ kgm}^{-3}$, the neutrons from the nuclei start dripping out, and this phenomena is called the *neutron drip*. These free neutrons then coexist in equilibrium with

electrons and nuclei [21]. However, the density of normal nuclear matter is $2.3 \times 10^{17} \text{kgm}^{-3}$, at higher densities, a dense gas of electrons protons and neutrons is formed due to the merged nuclei. At higher densities, there are two possibilities of β -decay,

$$n \longrightarrow p^+ + e^- + \bar{\nu}_e. \quad (3.3.7)$$

The decay will not occur if the states are already being occupied. Resulting in a number of neutrons present in the core. The Pauli's exclusion principle will become the reason to halt the decay.

$$\epsilon(n) < \epsilon(p) + \epsilon(e), \quad (3.3.8)$$

this expression tells us that all the neutrons with energy up to $\epsilon(n)$ are stabilized due to Pauli exclusion principle. Neutrons can beta decay if,

$$\epsilon(n) > \epsilon(p) + \epsilon(e). \quad (3.3.9)$$

At zero temperature, the equilibrium is obtained

$$\epsilon(n) = \epsilon(p) + \epsilon(e). \quad (3.3.10)$$

The chemical potential at zero temperature is the *Fermi energy* [15]. In order to find the concentration of neutrons, protons and electrons in the equilibrium in equation (3.3.10) can be found by the equation [21]

$$p_F = \left[\frac{3n}{8\pi} \right]^{\frac{1}{3}} h, \quad (3.3.11)$$

The neutrons and protons are non-relativistic when the density is of the order of nuclear density ρ_{nuc} , (where $\rho_{nuc} = 2.3 \times 10^{17} \text{kgm}^{-3}$ is the density of normal star) [21]. The relation between Fermi energies and non-relativistic neutrons and protons is

$$\epsilon(n) \approx m_n c^2 + \frac{p_F^2}{2m_n}, \quad (3.3.12)$$

and

$$\epsilon(p) \approx m_p c^2 + \frac{p_F^2}{2m_p}. \quad (3.3.13)$$

However, the electrons (less massive) become ultra-relativistic and the relation between their Fermi energy and momentum is

$$\epsilon(e) \approx p_F c. \quad (3.3.14)$$

The neutron star model is neutral, so we can put $n_e = n_p$, and find the concentration of neutrons and protons in ideal gas equilibrium. Putting the equations (3.3.12) and (3.3.13) in equation (3.3.10) we get

$$m_n c^2 + \frac{p_F(n)^2}{2m_n} = m_p c^2 + \frac{p_F(p)^2}{2m_p} + p_F(e)c. \quad (3.3.15)$$

Now putting the value of the Fermi momentum and $n_e = n_p$ [21], it becomes

$$m_n c^2 - m_p c^2 = \frac{1}{2m_p} \left(\frac{3n_p}{8\pi} \right)^{2/3} (h)^2 - \frac{1}{2m_n} \left(\frac{3n_n}{8\pi} \right)^{2/3} (h)^2 + \left(\frac{3n_e}{8\pi} \right)^{1/3} hc. \quad (3.3.16)$$

For a density $\rho = 2 \times 10^{17} \text{kgm}^{-3}$ we find, $n_e = n_p = n_n/200$. One electron per 200 neutrons is enough to prevent beta decay. So, neutrons are the dominant constituent in the neutron star.

3.4 Heavy Progenitors

The stars that are heavier than $8M_\odot$ are radically different, they carry their bulk with dignity until they can no longer cope and explode. Degeneracy will not set in till the elements up to iron are formed in the core of these stars because iron has the largest binding energy per nucleon. Now, after the all the elements till iron gets exhausted there will be no fusion reaction further. The star is on its track towards total destruction. The mass of this star is the reason of the continuous contraction in its core ($1-2M_\odot$), until $T_c \sim 5 \times 10^9 \text{ } ^\circ K$.

The electron density decreases so does the associated electron pressure that sustained the core. Free neutrons are formed in progressively large quantities, due to this increase in free neutrons, the core of the massive star start contracting. Now, as the core contracts rapidly and it will then collapse in about $0.1s$ until nuclear

densities are attained $10^{14} - 10^{15} \text{ g cm}^{-3}$, and the neutrons become degenerate. The core now consists of a degenerate neutron gas, with a small amount of electrons and protons in it. The neutron degeneracy pressure is sufficient to halt the further compression and a *neutron star* is formed. This is a giant atomic nucleus held together by gravity rather than the strong nuclear force.

3.5 General Relativity

To have an understanding of black holes and all other compact objects, we need to have the basic knowledge of general relativity and the four-vector formalism. Minkowski, in 1907, realized that special relativity could be reformulated in a more formal and mathematical approach, by the use of Four vectors, represented by x^μ , where the Greek index μ goes from 0 to 3. It has one time component x^0 and three spacial components x^i , where i is the Latin index running from 1 to 3.

In special relativity, there is a preferred family of observers called the inertial observers, where free particles can move with a uniform velocity. The Lorentz transformations relate all the inertial observers.

The interval ds is Lorentz invariant. The local measure of arc length ds is the metric here, which is given by the metric tensor $g_{\mu\nu}$. The arc length parameter is $ds = cd\tau$, where τ is the proper time. Now, 4-velocity v^μ can be obtained by the derivative of position vector with respect to this τ and the second derivative will give the acceleration A^μ . So, if an observer is moving without any force then the path that it follows will be the straightest possible path in spacetime. Thus, the directional derivative of the unit tangent vector should be zero along the path [26]. If t^μ is the path then the directional derivative of V^μ can be given as

$$\frac{dV^\mu}{ds} = t^\nu V^\mu{}_{;\nu} = t^\nu V^\mu{}_{,\nu} + t^\nu \Gamma_{\nu\rho}^\mu V^\rho, \quad (3.5.1)$$

where the comma and semi-colon represent the partial and co-variant derivatives, respectively with respect to the position vector.

The Christoffel symbols are given by

$$\Gamma_{\nu\rho}^{\mu} = \frac{1}{2}g^{\mu\sigma}(g_{\rho\sigma,\nu} + g_{\nu\sigma,\rho} - g_{\nu\rho,\sigma}). \quad (3.5.2)$$

$g^{\mu\sigma}$ is the inverse metric tensor i.e. $g^{\mu\sigma}g_{\nu\sigma} = \delta_{\nu}^{\mu}$. The condition for the straightest path becomes $dt^{\mu}/ds = 0$

$$\ddot{x}^{\mu} + \Gamma_{\nu\rho}^{\mu}\dot{x}^{\nu}\dot{x}^{\rho} = 0. \quad (3.5.3)$$

as $t^{\mu} = \dot{x}^{\mu}$. This is the *geodesic equation* and the path that follows this equation is called a *geodesic* [26]. The Christoffel symbols are the combination of the first derivatives but to find curvature we need second derivatives. Riemann's generalization of Gauss' theory for curved spaces gives the Riemann curvature tensor, which can be obtained by considering the difference of two covariant derivatives

$$\begin{aligned} Y_{;\rho;\pi}^{\mu} - Y_{;\pi;\rho}^{\mu} &= (Y_{;\rho}^{\mu} + \Gamma_{\mu}^{\nu\rho}Y^{\nu})_{;\pi} - (Y_{;\pi}^{\mu} + \Gamma_{\pi\nu}^{\mu}Y^{\nu})_{;\rho}, \\ Y_{;\rho;\pi}^{\mu} - Y_{;\pi;\rho}^{\mu} &= (\Gamma_{\nu\rho,\pi}^{\mu} - \Gamma_{\pi\nu,\rho}^{\mu})Y^{\nu} + (\Gamma_{\rho\sigma}^{\mu}\Gamma_{\pi\nu}^{\sigma} - \Gamma_{\pi\sigma}^{\mu}\Gamma_{\rho\nu}^{\sigma})Y^{\nu}, \\ Y_{;\rho;\pi}^{\mu} - Y_{;\pi;\rho}^{\mu} &= (\Gamma_{\nu\rho,\pi}^{\mu} - \Gamma_{\pi\nu,\rho}^{\mu} + \Gamma_{\rho\sigma}^{\mu}\Gamma_{\pi\nu}^{\sigma} - \Gamma_{\pi\sigma}^{\mu}\Gamma_{\rho\nu}^{\sigma})Y^{\nu}. \\ Y_{;\rho;\pi}^{\mu} - Y_{;\pi;\rho}^{\mu} &= R_{\nu\rho\pi}^{\mu}Y^{\nu}, \end{aligned}$$

where

$$R_{\nu\rho\pi}^{\mu} = \Gamma_{\nu\rho,\pi}^{\mu} - \Gamma_{\pi\nu,\rho}^{\mu} + \Gamma_{\rho\sigma}^{\mu}\Gamma_{\pi\nu}^{\sigma} - \Gamma_{\pi\sigma}^{\mu}\Gamma_{\rho\nu}^{\sigma}, \quad (3.5.4)$$

is the Riemann curvature tensor that measures the curvature of spacetime.

The Riemann curvature tensor possess the following properties;

It is skew-symmetric

$$R_{\alpha\nu\rho\pi} = -R_{\nu\alpha\rho\pi}, \quad R_{\alpha\nu\rho\pi} = -R_{\alpha\nu\pi\rho}. \quad (3.5.5)$$

It is symmetric when both the pair of indices are swapped

$$R_{\alpha\nu\rho\pi} = R_{\rho\pi\alpha\nu}. \quad (3.5.6)$$

It satisfies the first and second Bianchi identities

$$R_{\alpha\nu\rho\pi} + R_{\alpha\rho\pi\nu} + R_{\alpha\pi\nu\rho} = 0, \quad (3.5.7)$$

or we may write it as $R_{\alpha[\nu\rho\pi]} = 0$. The geodesic curvature can also be written in terms of derivatives as

$$R_{\alpha\nu\rho\pi;\mu} + R_{\alpha\nu\pi\mu;\rho} + R_{\alpha\nu\mu\rho;\pi} = 0, \quad (3.5.8)$$

which is known as *Bianchi identity*, and using the antisymmetric relation (3.5.5), we get

$$\nabla_{[\mu} R_{\alpha\nu]\rho\pi} = 0. \quad (3.5.9)$$

Now, from (3.5.5), raising α and then contracting on the first two indices gives

$$R_{\alpha\rho\pi}^{\alpha} = 0. \quad (3.5.10)$$

The contraction on first and last indices, however, give another tensor called *Ricci tensor*, which is symmetric.

$$R_{\alpha\nu} = R_{\alpha\nu\rho}^{\rho}. \quad (3.5.11)$$

A further contraction gives the trace of the Ricci tensor, the curvature scalar also called *Ricci scalar*.

$$R \equiv g^{\mu\nu} R_{\mu\nu} = R_{\mu}^{\mu}. \quad (3.5.12)$$

$$R_{\alpha\nu\rho\pi} = g_{\mu\alpha} R_{\nu\rho\pi}^{\mu}. \quad (3.5.13)$$

The covariant components of the curvature tensor in a coordinate system in which connection symbols vanish, $\Gamma_{\nu\pi}^{\mu} = 0$, (3.5.4) can be used to find

$$R_{\alpha\nu\rho\pi} = \frac{1}{2}(g_{\nu\rho,\pi\alpha} - g_{\alpha\rho,\pi\nu} + g_{\alpha\pi,\rho\nu} - g_{\nu\pi,\rho\alpha}). \quad (3.5.14)$$

Now, we will find a relation between the curvature and the distribution of matter (and energy).

The covariant derivatives of curvature scalar and the Ricci tensor can be used to find the Einstein's field equations. By using the Bianchi identities, the antisymmetric relations of the curvature tensor and raising some indices we finally get

$$\nabla_{\nu}(R^{\nu\rho} - \frac{1}{2}g^{\nu\rho}R) = 0. \quad (3.5.15)$$

The term in the parentheses is the *Einstein tensor*.

$$\varepsilon^{\alpha\beta} \equiv R^{\mu\nu} - \frac{1}{2}g^{\mu\nu}R. \quad (3.5.16)$$

Here, $\varepsilon^{\mu\nu}$ must be divergence-free and symmetric, so, the geometric quantity that fulfills these requirements is $\varepsilon^{\mu\nu} = g^{\mu\nu}$.

$$\varepsilon^{\mu\nu} \equiv R^{\mu\nu} - \frac{1}{2}Rg^{\mu\nu} = \kappa T^{\mu\nu}, \quad (3.5.17)$$

where $\varepsilon^{\mu\nu}$ is the tensor function of both the metric tensor and the curvature tensor and κ is the constant of proportionality. These are the Einstein's field equations, in which a cosmological constant was added later that came as the constant of integration.

$$R^{\mu\nu} - \frac{1}{2}Rg^{\mu\nu} - \Lambda g^{\mu\nu} = \kappa T^{\mu\nu}. \quad (3.5.18)$$

Here $T^{\mu\nu}$ is the stress-energy tensor which is given by

$$T^{\alpha\beta} = \rho u^\alpha u^\beta \sigma^{ij} \delta_i^\alpha \delta_j^\beta, \quad (3.5.19)$$

where u^α is the four-velocity, ρ is the density and σ^{ij} is the stress tensor. The relation between matter and curvature is already discussed through equation (3.5.17).

Now, finding the geodesic deviation, the position vector of the particle as seen by the observer is p^μ , along with the observers geodesic the acceleration vector must be the second directional derivative of this vector. So, d^2p^μ/ds^2 is the geodesic deviation, which can be obtained by considering \mathcal{L} as the Lie derivative along the curve, therefore it is necessary that

$$\mathcal{L}_t = 0. \quad (3.5.20)$$

$$\begin{aligned} t^\pi p^\mu_{;\pi} - p^\pi t^\mu_{;\pi} &= 0, \\ t^\pi p^\mu_{;\pi} &= p^\pi t^\mu_{;\pi}, \end{aligned} \quad (3.5.21)$$

The geodesic deviation is given by the acceleration vector \mathbf{A} as

$$A^\mu = \frac{d^2p^\mu}{ds^2}, \quad (3.5.22)$$

$$A^\mu = t^\rho [t^\pi p_{;\pi}^\mu]_{;\rho},$$

by using (3.5.21) we get

$$\begin{aligned} A^\mu &= t^\rho [t^\pi t_{;\pi}^\mu]_{;\rho}. \\ A^\mu &= t^\rho p_{;\rho}^\pi t_{;\pi}^\mu + t^\rho p^\pi t_{;\pi;\rho}^\mu, \\ A^\mu &= p^\rho t_{;\rho}^\pi t_{;\pi}^\mu + t^\rho p^\pi t_{;\pi;\rho}^\mu, \\ A^\mu &= p^\rho (t_{;\rho}^\pi t_{;\pi}^\mu)_{;\pi} - p^\rho t^\pi t_{;\pi;\rho}^\mu + t^\rho p^\pi t_{;\pi;\rho}^\mu, \\ A^\mu &= -p^\rho t^\pi t_{;\pi;\rho}^\mu + p^\rho t^\pi t_{;\pi;\rho}^\mu, \\ A^\mu &= t^\rho p^\pi t_{;\pi;\rho}^\mu + p^\rho t^\pi t_{;\pi;\rho}^\mu. \end{aligned}$$

Now, interchanging ρ and π in the first term we get

$$\begin{aligned} A^\mu &= t^\pi p^\rho t_{;\rho;\pi}^\mu + p^\rho t^\pi t_{;\pi;\rho}^\mu, \\ A^\mu &= R_{\nu\rho\pi}^\mu t^\nu p^\rho t^\pi. \end{aligned} \tag{3.5.23}$$

We get the connection between the curvature of spacetime and gravity [26].

3.6 The Classical Black holes

In the Newtonian theory of gravitation, the black holes (the objects that cannot be seen but attract matter) can be reviewed by considering a test particle of mass m . It is moving with an instantaneous speed v , around a body of mass M . Its potential and kinetic energies are

$$E_K = \frac{1}{2}mv^2, \tag{3.6.1}$$

$$E_P = \frac{GMm}{r}. \tag{3.6.2}$$

Here, r is the radial distance from the center of mass of the body m . If $E_K < E_P$, then the particle will move in bound closed orbits [26]. But if $E_K > E_P$ it will move freely in a hyperbolic orbit. The escape velocity is at the boundary between these two cases, it will move in a parabolic orbit and is called v_{esc} .

$$\frac{1}{2}Mv_{esc}^2 = \frac{GMm}{r}, \tag{3.6.3}$$

$$v_{esc} = \sqrt{\frac{2Gm}{r}}. \quad (3.6.4)$$

For an object, at the surface where $v_{esc} > c$, the strong gravitational attraction will be pulling things inside and is totally black, John Wheeler gave it the name of a black hole [26].

3.7 The Relativistic Black Holes

If the mass of the collapsed stellar core is greater than the maximum mass of a neutron star, a complete collapse will occur and the star becomes a *black hole* [21]. The maximum distance beyond which nothing can escape from a black hole is the *event horizon*.

In 1915, when the foundations of General Relativity (GR) was laid by Einstein, it became clear that gravity is not a force. It is rather, a distortion in space-time caused due to the presence of matter, which reduces to Newtonian theory in the weak field approximation. The size of the black hole depends on the mass of the collapsed stellar core. This size is known as the *Schwarzschild radius* r_s .

3.8 The Schwarzschild Black Hole

The reversal near a Schwarzschild black hole was calculated by Abramowicz, we are going to re-drive it in Chapter 4. Here, we need to see the Schwarzschild solution as it will be needed for the calculation. The Schwarzschild black hole is a static, spherically symmetric black hole, with mass M and zero charge and zero angular momentum. In 1916, Karl Schwarzschild presented a solution to Einstein field equations (vacuum solution), describing the gravitational field outside a spherical mass M . So, for the vacuum solution of the Einstein's field equations, with zero cosmological constant, where $T^{\mu\nu} = 0$, equation (3.5.18) becomes

$$R^{\mu\nu} - \frac{1}{2}Rg^{\mu\nu} = 0. \quad (3.8.1)$$

The most general solution for a spherically symmetric and static metric is given by [26]

$$ds^2 = e^{\nu(t,r)} dt^2 - e^{\lambda(t,r)} dr^2 - R^2(t,r) d\Omega^2, \quad (3.8.2)$$

where ν , λ , and R are the functions of time radial coordinates, and $d\Omega$ is

$$d\Omega^2 = d\theta^2 + \sin^2 \theta d\phi^2. \quad (3.8.3)$$

The spacetime considered here is static, so, the gravitational field does not vary with time (for a point mass). So, the metric becomes

$$ds^2 = e^{\nu(r)} dt^2 - e^{\lambda(r)} dr^2 - R^2(r) d\phi^2. \quad (3.8.4)$$

Now, $R^2(r)$ is taken as r^2 , our metric further reduces to

$$ds^2 = e^{\nu(r)} dt^2 - e^{\lambda(r)} dr^2 - r^2 d\Omega^2. \quad (3.8.5)$$

The metric tensor and its inverse can be given as

$$g_{\alpha\beta} = \begin{bmatrix} e^{\nu(r)} & 0 & 0 & 0 \\ 0 & -e^{\lambda(r)} & 0 & 0 \\ 0 & 0 & -r^2 & 0 \\ 0 & 0 & 0 & -r^2 \sin^2 \theta \end{bmatrix},$$

$$g^{\alpha\beta} = \begin{bmatrix} e^{-\nu(r)} & 0 & 0 & 0 \\ 0 & -e^{-\lambda(r)} & 0 & 0 \\ 0 & 0 & -1/r^2 & 0 \\ 0 & 0 & 0 & -1/r^2 \sin^2 \theta \end{bmatrix}.$$

The non-zero Christoffel symbols are [26]

$$\begin{aligned} \Gamma_{01}^0 &= \frac{1}{2}\nu', & \Gamma_{00}^1 &= \frac{1}{2}\nu'e^{\nu-\lambda}, & \Gamma_{11}^1 &= \frac{1}{2\lambda'}, \\ \Gamma_{22}^1 &= -re^{-\lambda}, & \Gamma_{33}^1 &= -r \sin^2 \theta e^{-\lambda}, & \Gamma_{12}^2 &= \frac{1}{r} = \Gamma_{13}^3, \\ & & \Gamma_{33}^2 &= -r \sin \theta \cos \theta, & \Gamma_{23}^3 &= \cot \theta. \end{aligned}$$

Einstein field equations for the vacuum solution reduces to

$$R_{\alpha\beta} = 0. \quad (3.8.6)$$

The non-zero components of $R_{\alpha\beta}$ are

$$R_{00} = \nu'' + \frac{1}{2\nu'}(\nu' - \lambda' + \frac{2\nu'}{r}) = 0, \quad (3.8.7)$$

$$R_{11} = -\nu'' - \frac{1}{\nu'}(\nu' - \lambda' - 2\frac{\lambda'}{r}) = 0, \quad (3.8.8)$$

$$R_{22} = 1 - e^{-\lambda} + \frac{1}{2r}(\lambda' - \nu')e^{-\lambda}, \quad (3.8.9)$$

$$R_{33} = R_{22}\sin^2\theta = 0. \quad (3.8.10)$$

Adding equations (3.8.7) and (3.8.8), we get

$$\frac{2\nu'}{r} + \frac{2\lambda'}{r} = 0, \quad (3.8.11)$$

$$\nu' + \lambda' = 0. \quad (3.8.12)$$

Integration yields

$$\nu + \lambda = \text{constant}. \quad (3.8.13)$$

So, we get

$$\nu(r) = -\lambda(r). \quad (3.8.14)$$

Now, putting the value of $\nu(r)$ in equation (3.8.9), we get

$$(-re^{-\lambda})' + 1 = 0. \quad (3.8.15)$$

Integrating and then dividing with r

$$e^{\nu(r)} = 1 + \frac{\alpha}{r}, \quad (3.8.16)$$

as $\nu = -\lambda$,

$$e^{-\lambda(r)} = 1 + \frac{\alpha}{r}, \quad (3.8.17)$$

where α is

$$\alpha = \frac{2Gm}{c^2}. \quad (3.8.18)$$

Here, we have taken $G = c = 1$. Now, the above equations become

$$e^{\nu(r)} = 1 - \frac{2m}{r}, \quad (3.8.19)$$

and

$$e^{-\lambda(r)} = 1 - \frac{2m}{r}. \quad (3.8.20)$$

Putting the values of $e^{\nu(r)}$ and $e^{-\lambda(r)}$ in equation (3.8.5) we get [26]

$$(ds)^2 = \left(1 - \frac{2M}{r}\right)(dt)^2 - \left(1 - \frac{2M}{r}\right)^{-1} (dr)^2 - (rd\theta)^2 - (r \sin \theta d\phi)^2. \quad (3.8.21)$$

This is the Schwarzschild black hole and its event horizon lies at $r_s = 2m$. As r approaches to infinity the metric reduces to Minkowski spacetime.

3.8.1 Singularities of Schwarzschild Black Hole

The following curvature invariants determine the singularities (two types) in Schwarzschild metric [26]

$$\begin{aligned} R_1 &= 0, \\ R_2 &= \frac{48G^2m^2}{c^4r^6}, \\ R_3 &= \frac{64G^3m^3}{c^6r^6}. \end{aligned}$$

The singularity that appears at $r = 0$ is essential while the singularity at $r = r_s$ is the coordinate singularity.

Chapter 4

Abramowicz's Relativistic Centrifugal Force

The relativistic effect: the centrifugal force attracts matter towards the center of the compact body, is discussed in this chapter. We will see that this effect does not depend on the motion of the reference frame, as explained in the Newtonian dynamics, but on the motion of particles along a curved path in space. We are going to find that in the presence of strong gravitational fields and closed circular photon trajectories in space, the centrifugal force seems to weaken i.e. it reverses its direction [16].

The change in the direction of the centrifugal force will be discussed through a formal approach using optical reference geometry which was first introduced by Abramowicz, Carter, and Lasota (1988) [16]. It is a conformal adjustment of the projected three-space. In optical reference geometry, the geodesic lines are the (spatial) projections of photon trajectories.

We have also discussed the role of the proper circumferential radius that is also called the radius of gyration \tilde{r} . It is the radial quantity whose gradient (defining the local outward direction) is important for the discussion of the dynamical properties and it has its origin with the specific angular momentum and angular velocity. The centrifugal force acts on the particle in the rotating frame if the photon trajectory and the particle's path in the global rest frame do not coincide. We will see that the

location of the circular path of the particle with respect to the photon path (circular trajectories), decides the direction of the centrifugal force i.e, whether it attracts or repels the rotation axis. However, on the circular photon path, the centrifugal force is zero.

4.1 The Centrifugal Force Reviewed in Two Different Descriptions

The force that appears to act outwards, away from the axis of rotation when reviewed in a rotating frame is the centrifugal force. Newton explained this description which deals with the rotation of the reference frame, in his *Principia* [27]. The second description stresses the motion of particles along a curved path in space.

Let us explain our first description which defines the Newtonian dynamics and uses Euclidean geometry of space. Consider the angular velocity of the rotating frame with respect to the absolute, or the global, rest frame, $\boldsymbol{\Omega}$, and the distance of the particle from the axis of rotation of the frame is, r . The centrifugal force acting on this particle in the rotating frame is

$$\mathbf{C} = m\boldsymbol{\Omega} \times (\mathbf{r} \times \boldsymbol{\Omega}). \quad (4.1.1)$$

This centrifugal force in classical mechanics can be obtained when the particle's motion, or the motion of a system of particles relative to a rotating coordinate frame, is discussed. The global rest frame can be determined with reference to the observations of distant galaxies [16]. All paths of these particles constitute a cylinder whose axis coincides with the axis of rotation of the frame [16, 28].

Let \mathbf{n} be the outward pointing normal on the circular paths as shown in Figure (4.1)

$$\mathbf{n} = \frac{\nabla r}{|(\nabla r) \cdot (\nabla r)|^{1/2}}. \quad (4.1.2)$$

The vector \mathbf{r} can be written as $\mathbf{r} = r\mathbf{n}$. The speed of the particle measured in global

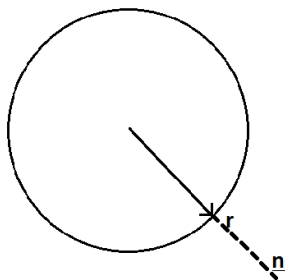


Figure 4.1: The outward pointing normal vector on the circular path.

rest frame is $v = |\boldsymbol{\Omega}|r$. Now, putting this in equation (4.1.1) and we get

$$\mathbf{C} = mr\Omega^2\mathbf{n} = \frac{mv^2}{r}\mathbf{n}. \quad (4.1.3)$$

In order to understand the dynamic situation in the co-rotating reference frame, let's discuss another description of the centrifugal force. The second description generalizes equation (4.1.1) to the motion along a non-circular trajectory [28]. Considering this, a non-circular trajectory may be composed of infinitesimally small circular fragments and a series of co-rotating reference frames associated with the particle's motion. The given trajectory $\mathbf{x} = \mathbf{x}(s)$, for the instantaneously co-rotating frames with a speed $v = v(s)$, can be defined by using the Frenet triad. A point is a zero-dimensional object and can be obtained by fixing all the coordinates. A curve is a one-dimensional object [26]. This means that the points on the curve will be generated by varying a single parameter. Thus, it can be shown by a variable position vector $\mathbf{x}(s)$ and s is the arc length parameter along the curve.

The Frenet frame explains the kinematics of the particle moving along the continuous, differentiable, curve in a three-dimensional Euclidean space. The tangent (to the curve) vector \mathbf{T} always points in the direction of motion as shown in the Figure (4.2).

$$\mathbf{T} = \frac{d\mathbf{x}}{ds}. \quad (4.1.4)$$

The first outward normal \mathbf{N} is defined as

$$\mathbf{N} = \Re \frac{d\mathbf{T}}{ds}. \quad (4.1.5)$$

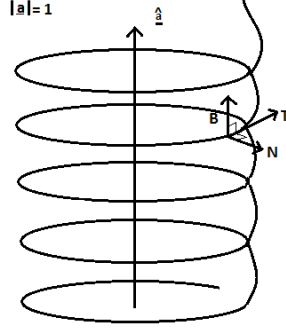


Figure 4.2: The Frenet frame is shown here. [26].

\mathfrak{R} is the geodesic curvature radius (it is the reciprocal of the curvature κ i.e. $1/\mathfrak{R}$ is called the first curvature). The second normal \mathbf{B} or the binormal unit vector is the cross product of \mathbf{T} and \mathbf{N} (see Figure (4.2)). The vectors \mathbf{T} , \mathbf{N} and \mathbf{B} satisfy the following orthogonality relations, known as Frenet triad [16, 28, 29].

$$\mathbf{T} = \mathbf{B} \times \mathbf{N}, \quad \mathbf{N} = \mathbf{T} \times \mathbf{B}, \quad \mathbf{B} = \mathbf{N} \times \mathbf{T}. \quad (4.1.6)$$

$$v = \frac{ds}{dt}, \quad \mathbf{T}v = \mathbf{v},$$

From equations (4.1.4) and (4.1.5), \mathbf{N} can also be written as

$$\mathbf{N} = \mathfrak{R} \frac{d\mathbf{T}}{ds} = \mathfrak{R} \left(\frac{d\mathbf{x}}{ds} \frac{d}{d\mathbf{x}} \right) \mathbf{T},$$

$$\mathbf{N} = \mathfrak{R}(T^\mu \nabla_\mu) \mathbf{T} = \mathfrak{R}(\mathbf{T} \cdot \nabla) \mathbf{T},$$

or

$$\mathbf{N} = \frac{1}{\kappa} (\mathbf{T} \cdot \nabla) \mathbf{T}, \quad (4.1.7)$$

where ∇ is the covariant derivative. The curvature κ measures the rate of change of unit tangent vector \mathbf{T} and how much the bending a curve can possess at a certain point [29]. The binormal unit vector can also be written as

$$\mathbf{N} = \mathbf{T} \times \mathbf{B},$$

$$\begin{aligned}\frac{d\mathbf{N}}{ds} &= \frac{d}{ds}(\mathbf{T} \times \mathbf{B}), \\ \frac{d\mathbf{N}}{ds} &= \frac{d\mathbf{T}}{ds} \times \mathbf{B} + \mathbf{T} \times \frac{d\mathbf{B}}{ds},\end{aligned}$$

where the rate of change of the binormal unit vector is $d\mathbf{B}/ds = -\tau\mathbf{N}$,

$$\begin{aligned}\frac{d\mathbf{N}}{ds} &= \left(\frac{1}{\mathfrak{R}}\mathbf{N}\right) \times \mathbf{B} + \mathbf{T} \times (-\tau\mathbf{N}), \\ \frac{d\mathbf{N}}{ds} &= \frac{1}{\mathfrak{R}}(-\mathbf{T}) - \tau(-\mathbf{B}), \\ \frac{d\mathbf{N}}{ds} &= \frac{-\mathbf{T}}{\mathfrak{R}} + \tau\mathbf{B}.\end{aligned}$$

So, we get

$$\mathbf{B} = \frac{1}{\tau} \left(\frac{d\mathbf{N}}{ds} + \frac{1}{\mathfrak{R}}\mathbf{T} \right), \quad (4.1.8)$$

where τ is the torsion which measures how much tendency is there in a curve to twist out of its osculating plane at each point [29].

For the arcs of minimum length, we are considering those curves where the curvature of the orthogonal projection of the curve onto the tangent is zero. When $1/\mathfrak{R} = 0$, the geodesic curvature becomes a geometrically straight line. The lines that coincide with photon trajectory are said to be the optically straight lines. The gyroscopically guided straight lines can be defined as the lines having the spin of the gyroscope initially tangent to it and will remain tangent throughout the motion of the gyroscope along the line.

The instantaneously co-rotating reference frame, for a particle moving along the curve $x(s)$ with speed $v(s)$, can be defined in terms of the angular velocity $\boldsymbol{\Omega}$, and angular displacement of the particle from the instantaneous rotation axis [30]. These two factors are

$$\boldsymbol{\Omega} = \left(\frac{v}{\mathfrak{R}}\right)\mathbf{B}, \quad (4.1.9)$$

$$\mathbf{r} = \mathfrak{R}\mathbf{N}. \quad (4.1.10)$$

From Newton's description (4.1.1), the Frenet formulas (4.1.7), (4.1.8) (4.1.9) and the equation (4.1.10), the centrifugal force in an instantaneously co-rotating reference frame can be found in terms of quantities that are defined in the global rest

frame.

$$\mathbf{C} \equiv m\boldsymbol{\Omega} \times (\mathbf{r} \times \boldsymbol{\Omega}), \quad (4.1.11)$$

$$\mathbf{C} = m \frac{v^2}{\mathfrak{R}} \mathbf{N}. \quad (4.1.12)$$

This is known as Huygen's description of the centrifugal force which becomes equivalent to Euclidean theory (of plane geometry), as the proper circumferential radius is equal to the geodesic curvature radius, $\mathfrak{R} = r$ and $\mathbf{N} = \mathbf{n}$. However, these two descriptions explain (physically) the same aspects of \mathbf{C} . The first description is based on the rotation of the reference frame with respect to the global rest frame while the second encounters the motion along the curved path ($\mathfrak{R} \neq \infty$) in space.

According to Newton's description, the necessary condition for the action of the centrifugal force (particularly in this frame) is that the reference frame must be the rotating frame i.e, $\boldsymbol{\Omega} \neq 0$ [28].

$$\mathbf{C} \neq 0 \Leftrightarrow \boldsymbol{\Omega} \neq 0, v \neq 0. \quad (4.1.13)$$

Huygens' description suggests that the particle's motion (with non-zero speed), along a non-straight path is the sufficient condition for the centrifugal force action [28].

$$\mathbf{C} \neq 0 \Leftrightarrow \mathfrak{R} \neq \infty, v \neq 0, \quad (4.1.14)$$

as $1/\mathfrak{R} = 0$ is a straight path in the spacetime. The proper circumferential radius r and the geodesic curvature radius \mathfrak{R} are different, $r \neq \mathfrak{R}$.

For simplicity, axially symmetric spaces; i.e. those which are symmetric around an axis of rotation are considered here. The circles in these spaces coincide with the Killing vector field, i.e. ξ^i , due to which this (axial) symmetry is generated.

4.2 Centrifugal Force in General Relativity

In this section, we are going to see which of the two descriptions of the centrifugal force is compatible with general relativity (the Newtonian description or the Huygens' description). Abramowicz, Carter, and Lasota developed the mathematical

formalism to find the centrifugal force. Consider a static and axially symmetric spacetime. Static spacetimes are those which cannot change over time and are irrotational. The second symmetry that we have considered is the one in which a body rotates with a constant angular velocity about a symmetry axis. These symmetries give rise to two-Killing vector fields. Time like vector field η_μ (open trajectories) and space-like vector field ξ_μ (closed trajectories). The Greek letters run from 0 to 3 and the Latin indices run from 1 to 3. The sign convention we have assumed here is $(-+++)$, spacelike vectors have positive and time like have negative lengths. The properties of these Killing vectors are

$$\nabla_{(\mu}\eta_{\nu)} = \nabla_{(\mu}\xi_{\nu)} = 0. \quad (4.2.1)$$

The round brackets show the symmetry and square brackets are used to show the anti-symmetric property. These Killing vectors are orthogonal

$$\boldsymbol{\eta} \cdot \boldsymbol{\xi} = \eta^\mu \xi_\mu = 0. \quad (4.2.2)$$

These Killing vectors $\boldsymbol{\eta}$ and $\boldsymbol{\xi}$ commute and give the following relations [31]. The requirement is that the metric (i.e. the tensor that describes the geometry) must remain invariant on the manifold, and hence is Lie transported. This provides the derivation of the equation

$$\mathcal{L}_\eta \boldsymbol{\xi} = \mathcal{L}_\xi \boldsymbol{\eta} = 0.$$

$$\xi^\nu \nabla_\nu \eta_\mu = \eta^\nu \nabla_\nu \xi_\mu,$$

also

$$\eta^\mu \nabla_\mu \eta_\nu = -\frac{1}{2} \nabla_\nu (\eta^\mu \eta_\mu),$$

$$\xi^\mu \nabla_\mu \xi_\nu = -\frac{1}{2} \nabla_\nu (\xi^\mu \xi_\mu).$$

$$\eta^\mu \nabla_\mu \xi_\nu = \xi^\mu \nabla_\mu \eta_\nu = -\frac{1}{2} \nabla_\nu (\xi^\mu \xi_\mu).$$

$$\nabla_{[\mu} \eta_{\nu]} = 0.$$

The scalar product of two vectors x^μ and y_μ is $\mathbf{x} \cdot \mathbf{y} \equiv x^\mu y_\mu$. Consider a static spacetime (in which if a light signal is sent from A to B , it is identical to the path

it travels back, from B to A). It follows the conditions defined above, and the observers themselves are static in that spacetime.

$$\eta_\mu = \nabla_\mu t = g_{tt}\delta_\mu^t, \quad (4.2.3)$$

$$g_{tt} = g_{00} = (\boldsymbol{\eta} \cdot \boldsymbol{\eta}). \quad (4.2.4)$$

Now, consider two observers that are infinitesimally close. The distance between them is the difference in the global time taken by the first observer in sending the signal to B and the moment of receiving it by B , dt .

$$\tilde{dl} = dt. \quad (4.2.5)$$

Here, $c = 1$. The metric of 3-dimensional space in terms of spacetime metric can be given by (the metric \tilde{g}_{ik} of optical reference geometry)

$$\tilde{g}_{ik} = -\frac{1}{(\boldsymbol{\eta} \cdot \boldsymbol{\eta})} g_{ik}. \quad (4.2.6)$$

$$\tilde{dl}^2 = \tilde{g}_{ik} dx^i dx^k. \quad (4.2.7)$$

$ds^2 = 0$ for the path of light.

Optical reference geometry defines a three dimensional projected space. The geometry of \tilde{g}_{ik} was introduced by Abramowicz. This was called optical reference geometry because the geodesic lines coincide with the photon path or the light rays in space [32]. The global time t and the optical reference geometry (\tilde{g}_{ik}) together define the global rest frame in space. The optical reference geometry is time *independent* and also axially symmetric. By the use of Fermat principle, we will elaborate optical reference geometry. The relativistic Fermat principle was found by Weyl for the static spacetimes. This principle states that the light follows the path of least time. According to this principle

$$\delta \int dt = 0, \quad (4.2.8)$$

the integral is taken between two fixed points on the photon trajectory. The minimal time and the minimal length can be explained by these formulas. The length is also minimal along the photon trajectory.

$$\delta \int dl = \delta \int (g_{ik} dx^i dx^k)^{\frac{1}{2}} = 0, \quad (4.2.9)$$

which shows that the light trajectories in space are geodesic lines in optical reference geometry. Let's start with the invariant definition of the outward direction with respect to the symmetry axis. The axial symmetry (ξ_μ) generates trajectories which are in a group of motions of circles with proper circumferential radii

$$r = \sqrt{(\boldsymbol{\xi} \cdot \boldsymbol{\xi})}. \quad (4.2.10)$$

The symmetry axis is $r = 0$ and the straight coaxial cylinders are defined as in the case of the Newtonian (previous section) outward normal in equation (4.1.2).

Now, the case of circular motion in a static, axially symmetric spacetime is considered. When a particle moves along a circle in space Figure (4.3), its four velocity is

$$v^\mu = z(\eta^\mu + \Omega \xi^\mu), \quad (4.2.11)$$

where v^μ is the linear combination of η^μ and ξ^μ [33]. Here, z is the normalization factor, which can be given as $z^{-2} = -[(\boldsymbol{\eta} \cdot \boldsymbol{\eta}) + \Omega^2(\boldsymbol{\xi} \cdot \boldsymbol{\xi})]$ and the orbital angular velocity of the particle is Ω . This equation (4.2.11) is the *Lorentz* form of four-velocity. The normalization factor can be found by using $(v^\alpha v_\alpha) = -1$, we get from equation (4.2.11)

$$-\frac{1}{z^2} = (\boldsymbol{\eta} \cdot \boldsymbol{\eta}) + \Omega^2(\boldsymbol{\xi} \cdot \boldsymbol{\xi}). \quad (4.2.12)$$

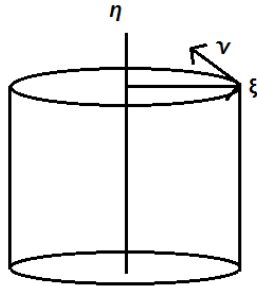


Figure 4.3: The four velocity \boldsymbol{v} of a particle in a static axially symmetric spacetime.

Assuming a stationary ($\Omega = 0$) observer,

$$u^\alpha = \frac{\eta^\alpha}{(\boldsymbol{\eta} \cdot \boldsymbol{\eta})^{1/2}}, \quad (4.2.13)$$

is the four-velocity of the observer. In Einstein's theory the four-velocity v^α of a particle is an absolute spacetime object. Let us denote u^α of an observer (an object), in an absolute spacetime. The proper (covariant) way to define the velocity \tilde{v}^β relative to the observer u^α is by the projection h_α^β of v^α into the local rest frame of the observer. In other simpler words the stationary observer equation (4.2.13) uniquely defines the global rest frame, and three-dimensional space in terms of projection tensor

$$h_\beta^\alpha = \delta_\beta^\alpha + u^\alpha u_\beta. \quad (4.2.14)$$

The three-dimensional metric can be defined as

$$\tilde{g}_{ik} = g_{ik} + u_i u_k. \quad (4.2.15)$$

Any geometrical quantity can be projected in the three-dimensional spacetime, (as an example we have the square of the orbital speed \tilde{v} in the projected three space which becomes the square of the projected velocity)

Now, consider for the relativistic speed of the particle which can be defined through the speed of the particle in Abramowicz's optical reference frame as

$$\tilde{v}^\beta \equiv h_\alpha^\beta v^\alpha, \quad (4.2.16)$$

$$\begin{aligned} \tilde{v}^2 &= \gamma^2 v^2 = \frac{\Omega^2 \tilde{r}^2}{1 - \Omega^2 \tilde{r}^2}, \\ \tilde{v} &= \gamma v = \frac{\Omega \tilde{r}}{\sqrt{1 - \Omega^2 \tilde{r}^2}}, \end{aligned} \quad (4.2.17)$$

taking $v = \Omega \tilde{r}$ the Lorentz speed (of the particle $0 \leq v^2 < 1$) and γ is the relativistic factor

$$\tilde{v} = \frac{v}{\sqrt{1 - v^2}}. \quad (4.2.18)$$

The quantity \tilde{r} is defined as the proper circumferential radius of the trajectories defined for the axially symmetric space. The geometrically \tilde{r} and its gradient $\nabla_\mu \tilde{r}$ is connected with the first normal vector \tilde{n} (pointing outward), and the geodesic curvature radius $\tilde{\mathfrak{R}}$.

$$\nabla_i \tilde{r} \equiv \frac{\partial \tilde{r}}{\partial x^i} \equiv \tilde{\nabla}_i \tilde{r}. \quad (4.2.19)$$

So,

$$\tilde{n}_\mu = \frac{\nabla_\mu \tilde{r}}{[(\nabla_\nu \tilde{r})(\nabla^\nu \tilde{r})]^{1/2}}, \quad (4.2.20)$$

$$\tilde{\mathfrak{R}} = \frac{\tilde{r}}{[(\nabla_\nu \tilde{r})(\nabla^\nu \tilde{r})]^{1/2}}. \quad (4.2.21)$$

Now, we can write acceleration in the general geodesic motion i.e, $a_\nu = v^\mu \nabla_\mu v_\nu$, by equation (4.2.17), which gives the four-velocity of the particle moving along the circular path

$$a_\nu = \frac{1}{2} \frac{\nabla_\nu (\boldsymbol{\eta} \cdot \boldsymbol{\eta}) + \Omega^2 \nabla_\nu (\boldsymbol{\xi} \cdot \boldsymbol{\xi})}{(\boldsymbol{\eta} \cdot \boldsymbol{\eta}) + \Omega^2 (\boldsymbol{\xi} \cdot \boldsymbol{\xi})}, \quad (4.2.22)$$

which can also be written in terms of speed of the particle measured in optical reference geometry \tilde{v} , geodesic curvature radius $\tilde{\mathfrak{R}}$ and first outward normal \tilde{n} as [34]

$$a_\nu = \frac{1}{2} \nabla_\nu \ln |(\boldsymbol{\eta} \cdot \boldsymbol{\eta})| - \frac{\tilde{v}^2}{\tilde{\mathfrak{R}}} \tilde{n}_\nu. \quad (4.2.23)$$

The free photon path c_{opt} (circular) is defined by two conditions $v^\mu v_\mu = 0$ and $a_\mu = 0$ by making use of equations (4.2.11), (4.2.22), (4.2.20), (4.2.21) and (4.2.23) as $\nabla_\mu \tilde{r} = 0$.

Now consider ($a_\nu \neq 0$), a non-geodesic motion in general a circular motion described by equation (4.2.11), (4.2.22) and (4.2.23). In order to keep moving along the circular path, the particle needs an external force like rocket thrust or the tension of a spring. For $a_\nu \neq 0$ we need a real force T_μ , except for the case of geodesic motion. The applied force becomes zero in the special case of geodesic motion. In GR, gravity appears as a part of acceleration, one can identify the *gravitational* and *centrifugal* parts of the acceleration vector. The gravitational force is being thought of independent of velocity, so, the first part in equation (4.2.23) is the gravitational force per unit mass and the second term is the centrifugal force per unit mass. For a particle moving with a rest mass m_0 , the centrifugal force becomes

$$C_\alpha = m_0 \frac{\tilde{v}^2}{\tilde{r}} \nabla_\alpha \tilde{r}. \quad (4.2.24)$$

The point clearly explains that C_α is always aligned with the direction of $\nabla_\alpha \tilde{r}$ (local outward direction). Even it becomes all misaligned with the global outward $\nabla_\alpha r$.

We will see in the next section that on the photon circular orbit ($r = 3M$) the acceleration is independent of velocity, in the vacuum Schwarzschild solution. $\nabla_\alpha \tilde{r}$ is zero there. The global and local directions interior to this point are directly opposite for the equatorial plane motion.

$$T_\nu = Tn_\nu = m\frac{1}{2}\nabla_\nu \ln |(\boldsymbol{\eta}\cdot\boldsymbol{\eta})| - m\frac{\tilde{v}^2}{\tilde{\mathfrak{R}}}\tilde{n}_\nu. \quad (4.2.25)$$

It means the real force is

$$T = m\left(\frac{1}{2}\tilde{U} - \frac{\tilde{v}^2}{\tilde{\mathfrak{R}}}\right), \quad (4.2.26)$$

where $\tilde{U} = \tilde{n}^\nu \nabla_\nu \ln |\boldsymbol{\eta}\cdot\boldsymbol{\eta}|$. There is no dependence on \tilde{v} , the speed of particle measured in the optical reference geometry. On a minimal circle, where $1/\tilde{R} = 0$. The description that matches with the general relativity is the Huygens' description. In the frame instantaneously co-rotating with the particle, the relativistic centrifugal force is

$$C_\mu = m\frac{\tilde{v}^2}{\tilde{\mathfrak{R}}}\tilde{n}_\mu, \quad (4.2.27)$$

\tilde{v} is the 3 dimensional component of velocity that is parallel to the von Zeipel cylinders. Now, we will discuss the behavior of the centrifugal force in strong gravitational fields.

Let us define the specific energy ε , that is the energy per unit mass and the specific angular momentum ℓ which is the angular momentum per unit mass, through invariant equations

$$\varepsilon = -\eta^\mu v_\mu, \quad (4.2.28)$$

and

$$L = \xi^\mu v_\mu, \quad (4.2.29)$$

So the specific angular momentum becomes

$$\ell = -\frac{1}{\varepsilon}\xi^\mu v_\mu. \quad (4.2.30)$$

From the Killing equation (4.2.1), it follows that ε and ℓ are constants of geodesic motion. In Schwarzschild coordinates (discussed in next section) one has

$$\eta^\mu = \delta_t^\mu, \quad \xi^\mu = \delta_\phi^\mu, \quad (4.2.31)$$

$$\eta^\mu \eta_\mu = g_{tt} = (g^{tt})^{-1}, \quad \xi^\mu \xi_\mu = g_{\phi\phi} = (g^{\phi\phi})^{-1}. \quad (4.2.32)$$

The specific angular momentum l and the orbital velocity Ω is linked through the relation

$$l = \Omega \tilde{r}^2. \quad (4.2.33)$$

The value \tilde{r} is the radius of gyration [35]

$$\tilde{r}^2 \equiv -\frac{(\boldsymbol{\xi} \cdot \boldsymbol{\xi})}{(\boldsymbol{\eta} \cdot \boldsymbol{\eta})}. \quad (4.2.34)$$

This defines the von Zeipel surfaces, i.e. those that coincide with the specific angular momentum $l = \text{constant}$ and angular velocity $\boldsymbol{\Omega} = \text{constant}$ surfaces in the isentropic and barotropic purely rotating general relativistic fluid configurations are called von Zeipel surfaces [36], which are defined by the von Zeipel parameter λ , having dimensions of length. We can write λ as

$$\lambda^2 = -\frac{g_{\phi\phi}}{g_{tt}}, \quad (4.2.35)$$

which is totally a geometric quantity. In this choice, the surfaces ($l = \text{constant}$) themselves become von Zeipel cylinders. So, the surfaces $l/\Omega = \text{constant}$ are known as von Zeipel cylinders, introduced by Abramowicz (1973). Defined in Euclidean geometry, these are straight cylinders, coaxial with the axis of rotation. Here, in the present case, we have taken the generalization of $\tilde{r}^2 = J/M\Omega$, \tilde{r} is the radius of gyration [35]

$$\tilde{r}^2 = \frac{l}{\Omega}, \quad (4.2.36)$$

is the ratio of specific angular momentum and angular velocity.

$$\tilde{r}^2 = -\frac{g_{\phi\phi}}{g_{tt}}. \quad (4.2.37)$$

The definition $l/\Omega = \text{constant}$, says that there exist critical circles at this certain point.

4.3 The Action of Centrifugal Force Reversal; The Rotosphere

Consider the vacuum Schwarzschild spacetime solution as explained in section (3.6)

$$(ds)^2 = -\left(1 - \frac{2M}{R}\right)(dt)^2 + \left(1 - \frac{2M}{R}\right)^{-1} (dR)^2 + (Rd\theta)^2 + (R \sin \theta d\phi)^2, \quad (4.3.1)$$

where M is the mass of the (central) compact object. The Killing vectors η_μ as explained in equations (4.2.3) and (4.2.4) can be given as

$$\eta_\mu = \nabla_\mu t, \quad \boldsymbol{\eta} \cdot \boldsymbol{\eta} = g_{tt} = g_{00} = -\left(1 - \frac{2M}{R}\right), \quad (4.3.2)$$

and ξ_μ can be written as

$$\xi_\mu = \nabla_\mu \phi, \quad \boldsymbol{\xi} \cdot \boldsymbol{\xi} = g_{\phi\phi} = g_{33} = R^2 \sin^2 \theta. \quad (4.3.3)$$

The orbital symmetry allows us to choose the angle for the orbital plane to be $\theta = \pi/2$. A Tetrad is the set of four locally defined linearly independent vectors $e_{\hat{a}} = e_{\hat{a}}^\mu \partial_\mu$, where $a = 0, 1, 2, 3$. The tetrad formalism is used to replace the choice of coordinate basis with a less restrictive local basis. The transformation of global to local coordinates is done with transformation matrices $e_{\hat{\beta}}^{\hat{\alpha}}$ and $e_{\hat{\beta}}^\alpha$. The components of transformation come from the metric tensor.

$$g_{\mu\nu} = e_{\hat{\mu}}^{\hat{\alpha}} e_{\hat{\nu}}^{\hat{\beta}} \eta_{\hat{\alpha}\hat{\beta}}. \quad (4.3.4)$$

The tetrad components of the spacelike vector \hat{a}^i can be defined as

$$\hat{a}^i = e_k^i a^k. \quad (4.3.5)$$

The orthonormal set of three vectors e_k^i .

$$e_{\hat{R}}^{\hat{R}} = \sqrt{g_{RR}} = \sqrt{\left(1 - \frac{2M}{R}\right)^{-1}} = \left(1 - \frac{2M}{R}\right)^{-1/2}, \quad (4.3.6)$$

$$e_{\hat{\theta}}^{\hat{\theta}} = R, \quad (4.3.7)$$

$$e_{\hat{\phi}}^{\hat{\phi}} = \sqrt{g_{\phi\phi}} = \sqrt{R^2 \sin^2 \theta} = R \sin \theta. \quad (4.3.8)$$

Now, defining χ as the angle between two curves say \mathbf{a} and \mathbf{b} , then for $\mathbf{a}\cdot\mathbf{b}$ we have

$$\cos \chi = a^{(R)}b^{(R)} + a^{(\theta)}b^{(\theta)} + a^{(\phi)}b^{(\phi)},$$

or

$$\cos \chi = a_{(R)}b_{(R)} + a_{(\theta)}b_{(\theta)} + a_{(\phi)}b_{(\phi)}.$$

In this case, $\cos \xi$ becomes

$$\cos \chi = n_{(R)}\tilde{n}_{(R)} + n_{(\theta)}\tilde{n}_{(\theta)} + n_{(\phi)}\tilde{n}_{(\phi)}. \quad (4.3.9)$$

The spacelike unit vector n^i defines the outward direction, which is away from the rotation axis. \tilde{n}^i is the unit vector defining the direction of the centrifugal force and is normal to the von Zeipel cylinders. Now in order to find its tetrad components, we have to first find the tetrad components of n^i . The straight cylinders can be given as $r^2 = (\boldsymbol{\xi}\cdot\boldsymbol{\xi}) = \text{constant}$. For the Schwarzschild solution, it takes the form $r^2 = R^2 \sin^2 \theta = \text{constant}$. We have the vector n^i , which is orthogonal to these cylinders, now we will find its tetrad components by using the equation (4.1.2).

$$n_{(R)} = \frac{\sin \theta (1 - 2M/R)^{1/2}}{|(1 - 2M/R \sin^2 \theta)|^{1/2}}, \quad (4.3.10)$$

$$n_{(\theta)} = \frac{\cos \theta}{|(1 - 2M/R \sin^2 \theta)|^{1/2}}, \quad (4.3.11)$$

$$n_{(\phi)} = 0. \quad (4.3.12)$$

Using equation (4.2.20), we can find the tetrad components of the normal \tilde{n}^i where \tilde{r} can be obtained by using $(\tilde{r}^2 = -(\boldsymbol{\xi}\cdot\boldsymbol{\xi})/\boldsymbol{\eta}\cdot\boldsymbol{\eta})$ equation (4.2.37). In Schwarzschild black hole, \tilde{r} becomes

$$\tilde{r}^2 = \frac{R^2 \sin^2 \theta}{(1 - 2M/R)}. \quad (4.3.13)$$

The tetrad components for \tilde{n}^i

$$\tilde{n}_{(R)} = \frac{\sin \theta (1 - 3M/R)}{|[(1 - 3M/R)^2 \sin^2 \theta + (1 - 2M/R) \cos^2 \theta]^{1/2}}, \quad (4.3.14)$$

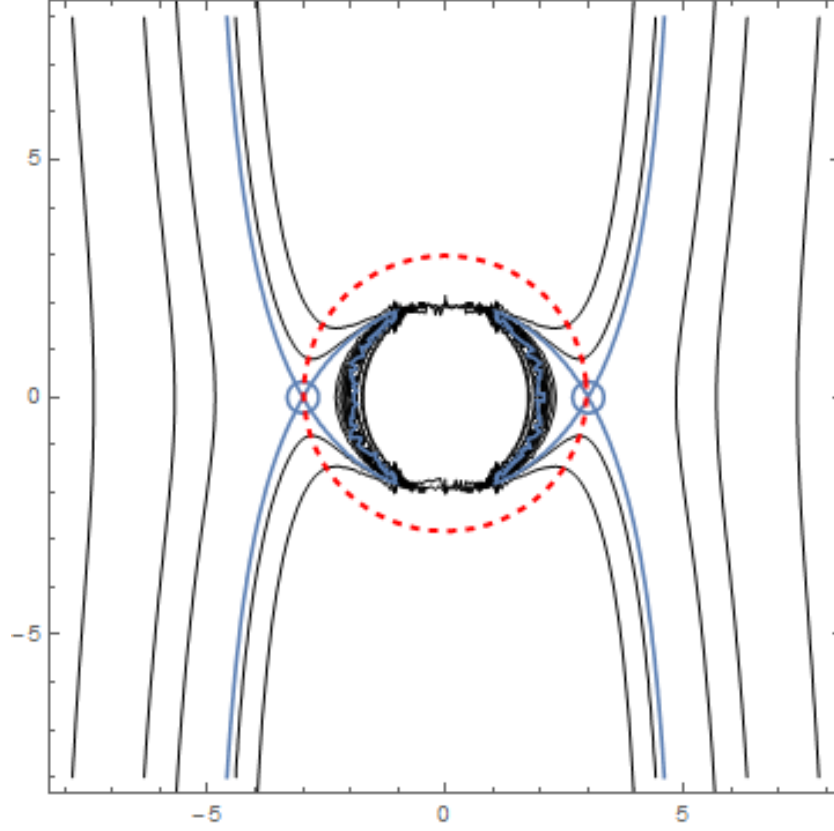


Figure 4.4: The equatorial section of von Zeipel cylinders in the Schwarzschild solution. Here, the dotted red colored circle show $R = 3M$ region and the black colored lines are the von Zeipel cylinders. Created using MATHEMATICA.

$$\tilde{n}_{(\theta)} = \frac{\cos \theta (1 - 2M/R)^{1/2}}{|[(1 - 3M/R)^2 \sin^2 \theta + (1 - 2M/R) \cos^2 \theta]^{1/2}|}, \quad (4.3.15)$$

$$\tilde{n}_{(\phi)} = 0. \quad (4.3.16)$$

The spacelike unit vector defines the outward (away from the rotation axis) normal on the straight cylinders. By the definition of centrifugal force, the direction is determined by equation (4.2.27), \tilde{n}^i , normal to von Zeipel cylinders.

Now, finding the angle χ , between the outward direction (away from the rotation axis) and that of the direction of the centrifugal force by equation (4.3.9), we get

$$\cos \chi(R, \theta) = \frac{\sin^2 \theta (1 - 3M/R) (1 - 2M/R)^{1/2} + \cos^2 \theta (1 - 2M/R)^{1/2}}{|(1 - 2M/R \sin^2 \theta)|^{1/2} |[(1 - 3M/R)^2 \sin^2 \theta + (1 - 2M/R) \cos^2 \theta]^{1/2}|}. \quad (4.3.17)$$

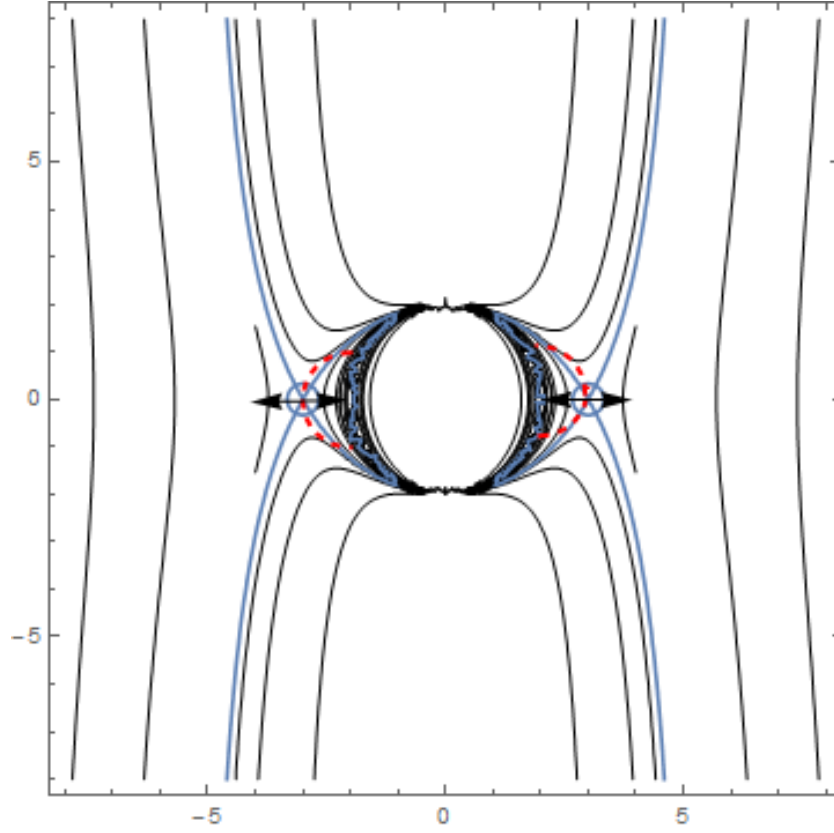


Figure 4.5: The red colored dotted region is the rotosphere, in which the centrifugal force would change direction. The blue colored lines represent the self-crossing von Zeipel cylinders and the center represents the gravitating star (black hole). Created using MATHEMATICA.

This can also be written as

$$\cos \chi(R, \theta) = \left[\left(1 - \frac{3M}{R} \right) \sin^2 \theta + \cos^2 \theta \right] S(R, \theta), \quad (4.3.18)$$

where $S(R, \theta)$ is

$$S(R, \theta) = \frac{(1 - 2M/R)^{1/2}}{|(1 - 2M/R \sin^2 \theta)|^{1/2} [(1 - 3M/R)^2 \sin^2 \theta + (1 - 2M/R) \cos^2 \theta]^{1/2}}. \quad (4.3.19)$$

From the above equation we get the centrifugal force reversal, i.e. the centrifugal force attracts towards the rotation axis. Here, in the entire region where $(R/3M) <$

$\sin^2 \theta$ is the region of $\cos \chi < 0$. Note that in the paper that has been reviewed, the equation (4.3.17) is explained only for the case where θ lies on the equatorial plane. The terms $\sin^2 \theta$ and $\cos^2 \theta$ that are present here, in equation (4.3.17), gives the general form of the solution when we are finding the angle between the outward normals of the straight cylinders and the von Zeipel cylinders (see [16]).

In Newtonian dynamics, the von Zeipel cylinders are straight cylinders, that strictly follow the cylindrical geometry. Far away from the gravitating center, both the types of cylinders have the same directions (the direction of their normals). The centrifugal force attracts towards the center in the region where $\sin^2 \theta > R/3M$. This region is the rotosphere [16, 30]. Figure (4.4) depicts the von Zeipel cylinders near the gravitating central body, i.e. Schwarzschild black hole. Straight cylinders follow cylindrical geometry, the normal to these cylinders and to von Zeipel cylinders can have opposite directions at a point where von Zeipel cylinders self-cross [30]. This is the same region where the existence of the rotosphere can be seen. Figure (4.5) shows the self-crossing von Zeipel cylinders and the rotosphere for the vacuum Schwarzschild solution ($\tilde{r} = 3\sqrt{3}M$). The point where the self-crossing occurs, the normal vector is undefined there. So, $\nabla_\alpha \tilde{r} = 0$. This tells us the existence of the closed photon orbit in space. The closed photon trajectory in Schwarzschild geometry can be seen when the von Zeipel cylinder $\tilde{r} = 3\sqrt{3}M$ self-crosses along the circle $R = 3M$, $\cos^2 \theta = 0$ as shown in the Figure (4.5). It can also be said as when there exists a closed circular photon orbit that corresponds to the unstable circular orbit, there must be von Zeipel cylinders (self-crossing their selves) and the rotosphere must exist.

The only condition for the rotosphere to exist is to see if there exists a self-crossing von Zeipel cylinder. The self-crossing von Zeipel cylinder can be seen in Figure (4.4) which occur at $\tilde{r} = 3\sqrt{3}M$.

The expression for the angle between the centrifugal force and outward normal (away from rotation axis) can be written as $\chi_0 = \chi(R, \theta = \pi/2)$

$$\cos \chi = \frac{1 - 3M/R}{|1 - 3M/R|} \begin{cases} +1, & \text{if } R > 3M \\ -1, & \text{if } R < 3M \end{cases}. \quad (4.3.20)$$

This form particularly, tells us the change in the direction of the centrifugal force [30]. At the center of the closed photon orbit the centrifugal force changes direction, it is attractive inside and repulsive outside this orbit. In Figures (4.4) and (4.5), the circle in the middle shows the self-gravitating object, which in our case is a Schwarzschild black hole. We can see self-crossing von Zeipel cylinders in both these Figures (4.4), and (4.5), which have been created using MATHEMATICA by transforming \tilde{r} into cylindrical polar co-ordinates.

4.3.1 The Effective Potential

Von Ziepel “cylinders” have a non-cylindrical behavior in spaces that are non-Euclidean i.e. hyperbolic, parabolic or elliptical. The motion of a photon in space whose velocity is v_μ , this is the component of velocity orthogonal to both the Killing vectors η_μ and ξ_μ . Let

$$\tilde{V}^2 = -\frac{(\eta\eta)(vv)}{L^2}. \quad (4.3.21)$$

The equation of motion for the photon is

$$\tilde{V}^2 = \tilde{h}^2 - V_{eff}, \quad (4.3.22)$$

where $\tilde{h} = E/L = constant$, is the impact parameter. Here, \tilde{h} is the impact parameter for the photon. The effective potential for the photon is $V_{eff} = 1/\tilde{r}^2$ [35].

At the extreme of effective potential $\nabla_\mu V_{eff} = 0$, the circular orbits of the photons are present.

As the direction of the unit normal vector to the von Zeipel cylinders $\tilde{\mathbf{n}}$ and the centrifugal force is same, see equation (4.2.27), the centrifugal force repulsion can be seen from the unstable circular orbits and attraction towards the stable circular orbits. The force does not act on the particles moving on the circular photon orbit. The stable circular orbits are those where the local minima correspond to

stable circular orbits. The unstable circular orbits are those where the local maxima correspond to unstable circular orbits. Figure (4.6) illustrates the effective potential (V_{eff}) for the motion of photon. Outside the star, the maximum corresponds to the unstable circular photon orbit.

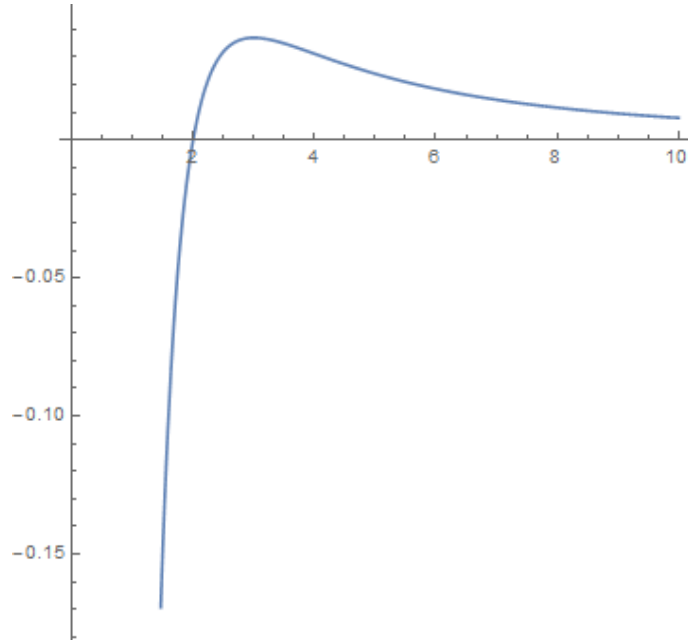


Figure 4.6: The effective potential for the motion of photon in the Schwarzschild solution's equatorial plane of a spherical constant density star is shown. Created using MATHEMATICA.

From equation (4.2.19) and (4.2.36) we have \tilde{n} to be a unit vector that is orthogonal to the von Zeipel cylinders. But this vector is not defined at the circular photon orbits, as $\nabla_{\mu}V_{eff} = -2\nabla_{\mu}\tilde{r}/\tilde{r}^3$, $\tilde{n}_{\mu} = 0/0 =$ (undefined), as we are dealing with $\tilde{r} = constant$ surfaces.

The unit vector \mathbf{n}' defines the outward radial direction r . Considering the equatorial plane of the Schwarzschild solution, if the scalar product ($nn' = +1$), the centrifugal force will point away from the rotation axis [30]. For ($nn' = -1$), the centrifugal force will point inwards (towards the axis of rotation). Now, on the equatorial plane of the exterior Schwarzschild solution, we can write for the scalar

product

$$(nn') = \frac{r - r_1}{|r - r_1|} \begin{cases} +1, & \text{if } r > r_1 = \frac{3}{2}R_G, \\ -1, & \text{if } r < r_1 = \frac{3}{2}R_G, \end{cases} \quad (4.3.23)$$

where R_G is the gravitational radius of the spherical gravitating body (Schwarzschild black hole or a compact star i.e. a neutron star). The geodesic curvature radius for the circles $r = \text{constant}$ is

$$\tilde{\mathfrak{R}} = \frac{r^2}{|r - r_1|}. \quad (4.3.24)$$

Thus, we have two cases, for $r = \frac{3}{2}R_G$ we have $\tilde{\mathfrak{R}} = \infty$. So, the centrifugal force would disappear there. For $R_G < r < \frac{3}{2}R_G$, the centrifugal force attracts towards the rotation axis. The centrifugal force is attractive towards the rotation axis between the two-photon orbits.

Bibliography

- [1] Norman K Glendenning. *Compact Stars: Nuclear Physics, Particle Physics and General Relativity*. Springer Science & Business Media, 2012.
- [2] Hans A Bethe. Energy production in stars. *Physical Review*, **55**:434–456, 1939.
- [3] Ganesan Srinivasan. *Life and Death of the Stars*. Springer, 2014.
- [4] Hale Bradt. *Astrophysics Processes: The Physics of Astronomical Phenomena*. Cambridge University Press, 2008.
- [5] Carl A Rouse. Stellar structure and stellar evolution another view. In *Physics and Contemporary Needs*, pages 379–403. Plenum Press, 1984.
- [6] Baidyanath Basu, Tanuka Chattopadhyay, and Sudhindra N Biswas. *An Introduction to Astrophysics*. PHI Learning Pvt. Ltd., 2010.
- [7] Terry L Smith, Michael D Reynolds, and Jay S Huebner. *Basic Astronomy Labs*. Prentice-Hall, 1996.
- [8] Remo Ruffini. Stellar structure and stellar evolution another view. In *Physics and Contemporary Needs*. Plenum Press, 1977.
- [9] Thanu Padmanabhan. *Theoretical Astrophysics: Stars and Stellar Systems*. Cambridge University Press, 2001.
- [10] Dan Maoz. *Astrophysics in a Nutshell*. Princeton University Press, 2007.

- [11] Krishna D Abhyankar. *Astrophysics: Stars and Galaxies*. Universities Press, 2002.
- [12] Marc L Kutner. *Astronomy: A Physical Perspective*. Cambridge University Press, 2003.
- [13] Jay M Pasachoff. *Astronomy: From the Earth to Universe*. Harcourt Brace College Publishers, 1982.
- [14] Subrahmanyan Chandrasekhar. *An Introduction to the Study of Stellar Structure*. Courier Corporation, 1957.
- [15] Stuart L Shapiro and Saul A Teukolsky. *Black Holes, White Dwarfs, and Neutron Stars: The Physics of Compact Objects*. John Wiley & Sons, 2008.
- [16] Marek A Abramowicz and A R Prasanna. Centrifugal force reversal near a Schwarzschild black hole. *Monthly Notices of the Royal Astronomical Society*, **245**:720–728, 1990.
- [17] Paulo C Freire and A A Da Costa. Centrifugal forces and optical geometry in neutron stars. *Astrophysics and Space Science*, **272**:275–282, 2000.
- [18] Marek A Abramowicz, W Kluźniak, and Jean-Pierre Lasota. The centrifugal force reversal and X-Ray bursts. *Astronomy & Astrophysics*, **374**:L16–L18, 2001.
- [19] Morse M Phillips. *Thermal Physics*. W A Benjamin, 2013.
- [20] Daniel V Schroeder. *An Introduction to Thermal Physics*. Addison Wesley Longman, 1999.
- [21] Anthony C Phillips. *The Physics of Stars*. John Wiley & Sons, 2013.
- [22] Burnell B Jocelyn and Antony Hewish. Angular size and flux density of the small source in the Crab Nebula at 81.5 mc/s. *Nature*, **213**:1214–1216, 1967.

- [23] Antony Hewish. Pulsars and high density physics. *Science*, **188**:1079–1083, 1975.
- [24] Thomas Gold. Rotating neutron stars and the nature of pulsars. *Nature*, **221**:25–27, 1969.
- [25] Cocke W John, John M Disney, and Joseph Taylor. Discovery of optical signals from pulsar NP 0532. *Nature*, **221**:525–527, 1969.
- [26] Asghar Qadir. *Einstein's General Theory of Relativity*. (Under preparation).
- [27] Isaac Newton and Alberto Pala. *Principi Matematici Della Filosofia Naturale*. Union Tipografica-Editrice Torinese, 1965.
- [28] Marek A. Abramowicz. Unexpected properties of the centrifugal force. In *Proceedings, Summer School in High-energy Physics and Cosmology: Trieste, Italy 26 June-18 August, 1989*, pages 586–609, 1990.
- [29] David Kay. *Schaum's Outline of Tensor Calculus*. McGraw Hill Professional, 1988.
- [30] Marek A Abramowicz. Centrifugal force: A few surprises. *Monthly Notices of the Royal Astronomical Society*, **245**:733–746, 1990.
- [31] Luciano Rezzolla and Olindo Zanotti. *Relativistic Hydrodynamics*. Oxford University Press, 2013.
- [32] Marek A Abramowicz. Relativity of inwards and outwards: An example. *Monthly Notices of the Royal Astronomical Society*, pages 710–718, 1992.
- [33] Marek A Abramowicz. Velocity, acceleration and gravity in general relativity. *arXiv preprint arXiv:1608.07136*, 2016.
- [34] Asghar Qadir and J Quamar. Pseudo-Newtonian potentials. *Europhysics Letters*, **2**:422–425, 1986.

- [35] Marek A Abramowicz, Jaffery C Miller, and Stuchilk Z. Concept of radius of gyration in general relativity. *Physical Review D*, **47**:1440–1447, 1993.
- [36] Sandip K Chakrabarti. Von Zeipel surfaces. *Monthly Notices of the Royal Astronomical Society*, **245**:747–748, 1990.